



HAL
open science

Adaptive Detection of Coherent Radar Targets in the Presence of Noise Jamming

Pia Addabbo, Olivier Besson, Danilo Orlando, Giuseppe Ricci

► **To cite this version:**

Pia Addabbo, Olivier Besson, Danilo Orlando, Giuseppe Ricci. Adaptive Detection of Coherent Radar Targets in the Presence of Noise Jamming. *IEEE Transactions on Signal Processing*, 2019, 67 (24), pp.6498-6510. 10.1109/TSP.2019.2954499 . hal-02613952

HAL Id: hal-02613952

<https://hal.science/hal-02613952>

Submitted on 20 May 2020

HAL is a multi-disciplinary open access archive for the deposit and dissemination of scientific research documents, whether they are published or not. The documents may come from teaching and research institutions in France or abroad, or from public or private research centers.

L'archive ouverte pluridisciplinaire **HAL**, est destinée au dépôt et à la diffusion de documents scientifiques de niveau recherche, publiés ou non, émanant des établissements d'enseignement et de recherche français ou étrangers, des laboratoires publics ou privés.



Open Archive Toulouse Archive Ouverte (OATAO)

OATAO is an open access repository that collects the work of some Toulouse researchers and makes it freely available over the web where possible.

This is an author's version published in: <https://oatao.univ-toulouse.fr/25981>

Official URL : <https://doi.org/10.1109/TSP.2019.2954499>

To cite this version :

Addabbo, Pia and Besson, Olivier and Orlando, Danilo and Ricci, Giuseppe Adaptive Detection of Coherent Radar Targets in the Presence of Noise Jamming. (2019) IEEE Transactions on Signal Processing, 67 (24). 6498-6510. ISSN 1053-587X

Any correspondence concerning this service should be sent to the repository administrator:

tech-oatao@listes-diff.inp-toulouse.fr

Adaptive Detection of Coherent Radar Targets in the Presence of Noise Jamming

Pia Addabbo , Member, IEEE, Olivier Besson , Danilo Orlando , Senior Member, IEEE, and Giuseppe Ricci , Senior Member, IEEE

Abstract—In this paper, we devise adaptive decision schemes to detect targets competing against clutter and smart noise-like jammers (NLJ) which illuminate the radar system from the sidelobes. Specifically, the considered class of NLJs generates a pulse of noise (noise cover pulse) that is triggered by and concurrent with the received uncompressed pulse in order to mask the skin echo and, hence, to hide the true target range. The detection problem is formulated as a binary hypothesis test and two different models for the NLJ are considered. Then, ad hoc modifications of the generalized likelihood ratio test are exploited where the unknown parameters are estimated by means of cyclic optimization procedures. The performance analysis is carried out using simulated data and proves the effectiveness of the proposed approach for both situations where the NLJ is either active or switched off.

Index Terms—Adaptive radar detection, alternating estimation, generalized likelihood ratio test, electronic countermeasures, electronic counter-countermeasures, noise cover pulse, noise-like jammers.

I. INTRODUCTION

ELECTRONIC countermeasures (ECMs) are active techniques aimed at protecting a platform from being detected and tracked by the radar [1]. This is accomplished through two approaches: masking and deception. Noncoherent jammers or noise-like jammers (NLJs) attempt to mask targets generating nondeceptive interference which blends into the thermal noise of the radar receiver. As a consequence, the radar sensitivity is degraded due to the increase of the constant false alarm rate threshold which adapts to the higher level of noise [1], [2]. In addition, this increase makes it more difficult to discover that jamming is taking place [3], [4]. On the other hand, the coherent jammers (CJs) transmit low-duty cycle signals intended to inject false information into the radar processor. Specifically, they are capable of receiving, modifying, amplifying, and retransmitting

the radar's own signal to create false targets maintaining radar's range, Doppler, and angle far away from the true position of the platform under protection [1]–[3], [5].

Nowadays, radar designers have developed defense strategies referred to as electronic counter-countermeasures (EC-CMs) which are aimed at countering the effects of the enemy's ECM and eventually succeeding in the intended mission. Such techniques can be categorized as antenna-related, transmitter-related, receiver-related, and signal-processing-related depending on the main radar subsystem where they take place [3]. The reader is referred to [3, and references therein] for a detailed description of the major ECCM techniques.

The first line of defense against jamming is represented by the radar antenna, whose beam pattern can be suitably exploited and/or shaped to eliminate sidelobe false targets or to attenuate the power of NLJs entering from the antenna sidelobes. In this context, famous antenna-related techniques capable of preventing jamming signals from entering through the radar sidelobes are the so-called sidelobe blanking (SLB) and sidelobe canceling (SLC) [6]. In particular, suppression of NLJs can be accomplished via an SLC system. SLC uses an array of auxiliary antennas to adaptively estimate the direction of arrival and the power of the jammers and, subsequently, to modify the receiving pattern of the radar antenna placing nulls in the jammers' directions. SLB and SLC can be jointly used to face with NLJs and CJs contemporaneously impinging on the sidelobes of the victim radar [7]. In [6] it is also shown that a data dependent threshold, based on [8], outperforms a cascade of SLC and SLB stages. The detector proposed in [8] is a special case of the more general class of tunable (possibly space-time) detectors which have been shown to be an effective means to attack detection of mainlobe targets or rejection of CJs notwithstanding the presence of NLJs and clutter [8]–[20]. As a matter of fact, such solutions can be viewed as signal-processing-related ECCMs. A way to design tunable receivers relies on the so-called two-stage architecture; such schemes are formed by cascading two detectors (usually with opposite behaviors in terms of selectivity): the overall one declares the presence of a target in the cell under test only when data survive both detection thresholdings [9]–[12], [16]–[20]. Such detectors can also be used as classifiers: in this case, the first stage is less selective than the second one and it is used to discriminate between the null hypothesis and the alternative that a structured signal is present. In case of detection, the second stage is aimed at discrimination between mainlobe and sidelobe signals, as explicitly shown in [17] for the adaptive sidelobe

The associate editor coordinating the review of this manuscript and approving it for publication was Dr. Xavier Mestre. (Corresponding author: Danilo Orlando.)

P. Addabbo is with the Università degli Studi “Giustino Fortunato,” 82100 Benevento, Italy (e-mail: p.addabbo@unifortunato.eu).

O. Besson is with the Institut Supérieur de l'Aéronautique et de l'Espace, University of Toulouse, Toulouse 31055, France (e-mail: olivier.besson@isae-supaero.fr).

D. Orlando is with the Università degli Studi “Niccolò Cusano,” 00166 Roma, Italy (e-mail: danilo.orlando@unicusano.it).

G. Ricci is with the Dipartimento di Ingegneria dell'Innovazione, Università del Salento, 73100 Lecce, Italy (e-mail: giuseppe.ricci@unisalento.it).

Digital Object Identifier 10.1109/TSP.2019.2954499

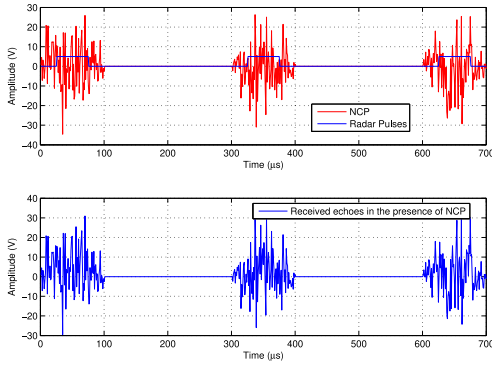


Fig. 1. Operating principle of NCP.

blanker (ASB). Adaptive detection and discrimination between useful signals and CJs in the presence of thermal noise, clutter, and possible NLJ has also been addressed in [21]. Therein the CJ is assumed to belong to the orthogonal complement of the space spanned by the nominal steering vector (after whitening by the true covariance matrix of the composite disturbance). This approach, based on a modified adaptive beamformer orthogonal rejection test (ABORT), see also [20], [22], allows to investigate the discrimination capabilities of adaptive arrays when the CJ is not necessarily confined to the “sidelobe beam pattern,” but might also be a mainlobe deception jammer. Another approach to deal with CJ is presented in [23], [24], where the CJ is modeled exploiting the subspace paradigm. A network of radars can be exploited to combat ECM signals. In this case, it is reasonable that, for a given CUT, only a subset of the radars receives ECM signals (CJs) as considered in [25].

Herein, we address adaptive detection in presence of noise cover pulse (NCP) jamming. The NCP is an ECM technique belonging to the class of noise-like jamming. Specifically, this kind of ECM generates a pulse of noise that is triggered by and concurrent with the received uncompressed pulse (see Fig. 1). To this end, several received radar pulses are used to estimate the pulse width (PW) and the pulse repetition interval (PRI) to predict the arrival time instant of the next pulse of the victim radar. The transmitted noise power is strong enough to mask the skin echo even after the radar performs the pulse compression, which is used to enhance the range resolution. It follows that, since the length of the transmitted pulse is much higher than the duration of a range bin, the NCP creates an extended-range return spread over many range bins that hides the true target range. Thus, it becomes of vital importance for a radar system to counteract the effects of an NCP attack. An ECCM technique against NCP is represented by the cover pulse channel (CPC) [26], which consists in using an auxiliary physical channel to track the NCP transmission rather than the skin return from the target. The main drawbacks of this technique are the degradation of the high-range resolution associated with the narrow pulses which result from the compression process and the exploitation of additional hardware resources. In order to overcome such limitations, in this paper we devise a signal-processing-related ECCM capable of detecting targets which compete against a NCP, while satisfying the original system requirements on range

resolution. Besides, the proposed solution by its nature can reside in the signal processing unit of the system without the need of additional hardware. From a mathematical point of view, we formulate the detection problem as a binary hypothesis test where primary data (namely those containing target returns) are formed by a set of range bins which is representative of the uncompressed pulse length and such that target return is located in only one bin whereas all the primary range bins are contaminated by the NCP. As for the NCP, we consider two models. In the first case, the NCP is represented as a rank-one modification of the interference covariance matrix (ICM), while in the second case the presence of the NCP is accounted for by including a deterministic structured component in all the range bins. Moreover, we assume that a set of training samples are available to estimate the clutter and noise components of the ICM. These data are collected using a suitable number of guard cells surrounding those under test and related to the uncompressed pulse length. Then, we derive adaptive architectures exploiting *ad hoc* modifications of the generalized likelihood ratio test (GLRT) design criterion where the unknown parameters are estimated resorting to an alternating procedure. Specifically, we leverage the cyclic optimization paradigm described in [27]–[29]. Finally, we present numerical examples which highlight the effectiveness of the proposed solutions also in comparison with existing architectures which are somehow compatible with the considered problem.

The remainder of the paper is organized as follows: next section is devoted to the problem formulation and to the description of the two different models for the NCP. Section III contains the derivation of the detection architectures, whereas Section IV provides the performance assessment of the detectors (also in comparison to natural competitors). Concluding remarks and future research tracks are given in Section V.

A. Notation

In the sequel, vectors and matrices are denoted by boldface lower-case and upper-case letters, respectively. The symbols $\det(\cdot)$, $\text{Tr}(\cdot)$, $\text{etr}\{\cdot\}$, $(\cdot)^*$, $(\cdot)^T$, $(\cdot)^\dagger$ denote the determinant, trace, exponential of the trace, complex conjugate, transpose, and conjugate transpose, respectively. As to numerical sets, \mathbb{R} is the set of real numbers, $\mathbb{R}^{N \times M}$ is the Euclidean space of $(N \times M)$ -dimensional real matrices (or vectors if $M = 1$), \mathbb{C} is the set of complex numbers, and $\mathbb{C}^{N \times M}$ is the Euclidean space of $(N \times M)$ -dimensional complex matrices (or vectors if $M = 1$). \mathbf{I}_N stands for the $N \times N$ identity matrix, while $\mathbf{0}$ is the null vector or matrix of proper dimensions. Let $f(\mathbf{x}) \in \mathbb{R}$ be a scalar-valued function of vector argument, then $\partial f(\mathbf{x})/\partial \mathbf{x}$ denotes the first derivative of $f(\cdot)$ with respect to \mathbf{x} arranged in a column vector. The Euclidean norm of a vector is denoted by $\|\cdot\|$. The (k, l) -entry (or l -entry) of a generic matrix \mathbf{A} (or vector \mathbf{a}) is denoted by $\mathbf{A}(k, l)$ (or $\mathbf{a}(l)$). Finally, we write $\mathbf{x} \sim \mathcal{CN}_N(\mathbf{m}, \mathbf{M})$ if \mathbf{x} is an N -dimensional complex normal vector with mean \mathbf{m} and positive definite covariance matrix \mathbf{M} .

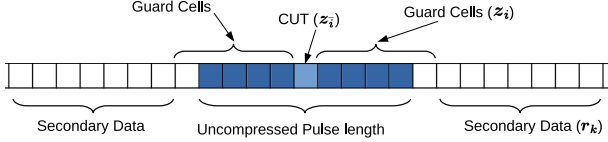


Fig. 2. Range bins partitioning.

II. PROBLEM STATEMENT

Assume that the radar is equipped with a uniformly-spaced linear array (ULA) of N identical and isotropic sensors with inter-element distance equal to $\lambda/2$, λ being the wavelength corresponding to the radar carrier frequency. For each sensor, the incoming signal is downconverted to baseband and, then, convolved with a conjugate time-reversed copy of the transmitted waveform (matched filter). The output of this filter is sampled to form the range bins of the area under surveillance. Thus, each range bin is represented by an N -dimensional complex vector. In what follows, we assume that the signal received from the cell under test (CUT) can be interference only, i.e., thermal noise, clutter, and a possible NCP jamming, or a noisy version of the signal backscattered by a coherent target.

As stated in Section I, the NCP is an ECM technique belonging to the class of noise-like jamming. Commonly, on the radar side, the action of the NCP jammer leads to an increase of the noise level over many range bins hiding the true target range.

In order to model this situation, we denote by \bar{i} the integer indexing the CUT and by $\Omega = \{\bar{i} - H_1, \dots, \bar{i} + H_2\}$ a set of integers indexing the range bins contaminated by the NCP jammer which also includes the CUT. The number of range bins after and before the CUT that are contaminated by the NCP jammer is not necessarily the same due to possible uncertainty in the PW and PRI estimates. Moreover, such parameters are not known at the radar receiver, but an educated guess is possible. Thus, in the following we do not address the problem of determining H_1 and H_2 , but assume that H_1 and H_2 and, hence, $H = H_1 + H_2 + 1$, the number of contaminated cells, is known. Additionally, we assume that a set of $K \geq N$ secondary data, representative of thermal noise plus clutter only, is collected by the radar using a number of guard cells reflecting the length of the uncompressed pulse (see Fig. 2).

With the above model in mind, denote by $\mathbf{z}_{\bar{i}} \in \mathbb{C}^{N \times 1}$, $\mathbf{z}_i \in \mathbb{C}^{N \times 1}$ with $i \in \Omega \setminus \{\bar{i}\}$, and $\mathbf{r}_k \in \mathbb{C}^{N \times 1}$ with $k = 1, \dots, K$, the vector containing the returns from the CUT, the vectors contaminated by NCP jammer, but free of target components, and the secondary data, respectively. For further developments we assume that such vectors are statistically independent. Then, the problem of detecting the possible presence of a coherent return from a given cell is formulated in terms of the following hypothesis test

$$\begin{cases} \mathcal{H}_0 : \begin{cases} \mathbf{z}_{\bar{i}} \sim \mathcal{CN}_N(\mathbf{0}, \mathbf{M} + \mathbf{q}\mathbf{q}^\dagger), \\ \mathbf{z}_i \sim \mathcal{CN}_N(\mathbf{0}, \mathbf{M} + \mathbf{q}\mathbf{q}^\dagger), & i \in \Omega \setminus \{\bar{i}\}, \\ \mathbf{r}_k \sim \mathcal{CN}_N(\mathbf{0}, \mathbf{M}), & k = 1, \dots, K, \end{cases} \\ \mathcal{H}_1 : \begin{cases} \mathbf{z}_{\bar{i}} \sim \mathcal{CN}_N(\alpha\mathbf{v}(\theta_T), \mathbf{M} + \mathbf{q}\mathbf{q}^\dagger), \\ \mathbf{z}_i \sim \mathcal{CN}_N(\mathbf{0}, \mathbf{M} + \mathbf{q}\mathbf{q}^\dagger), & i \in \Omega \setminus \{\bar{i}\}, \\ \mathbf{r}_k \sim \mathcal{CN}_N(\mathbf{0}, \mathbf{M}), & k = 1, \dots, K, \end{cases} \end{cases} \quad (1)$$

where

- $\alpha \in \mathbb{C}$ is an unknown deterministic factor accounting for target response and channel effects;
- $\mathbf{v}(\theta_T) = \frac{1}{\sqrt{N}} [1 e^{j\pi \sin(\theta_T)} \dots e^{j\pi(N-1) \sin(\theta_T)}]^T \in \mathbb{C}^{N \times 1}$ is the known steering vector of the target with θ_T the angle of arrival of the target¹: in the following, for brevity, we omit the dependence of \mathbf{v} on θ_T ;
- $\mathbf{M} \in \mathbb{C}^{N \times N}$ is the unknown positive definite covariance matrix of thermal noise plus clutter;
- $\mathbf{q} \in \mathbb{C}^{N \times 1}$ is an unknown vector representing the contribution to the noise covariance matrix of the NCP jamming.

Some definitions that will be used in the next developments for problem (1) are now in order. Let $\mathbf{Z}_{\Omega, \bar{i}} = [\mathbf{z}_{\bar{i}-H_1} \dots \mathbf{z}_{\bar{i}-1} \mathbf{z}_{\bar{i}+1} \dots \mathbf{z}_{\bar{i}+H_2}]$, $\mathbf{Z}_{\alpha, \bar{i}} = [\mathbf{z}_{\alpha, \bar{i}} \mathbf{Z}_{\Omega, \bar{i}}]$ with $\mathbf{z}_{\alpha, \bar{i}} = \mathbf{z}_{\bar{i}} - \alpha\mathbf{v}$, and $\mathbf{Z}_{\bar{i}} = [\mathbf{z}_{\bar{i}} \mathbf{Z}_{\Omega, \bar{i}}]$. Then, the probability density functions (PDFs) of $\mathbf{Z}_{\bar{i}}$ under \mathcal{H}_0 and \mathcal{H}_1 are given by

$$f_0(\mathbf{Z}_{\bar{i}}; \mathbf{q}, \mathbf{M}) = \frac{1}{[\pi^N \det(\mathbf{M} + \mathbf{q}\mathbf{q}^\dagger)]^H} \times \text{etr} \left\{ -(\mathbf{M} + \mathbf{q}\mathbf{q}^\dagger)^{-1} \mathbf{Z}_{\bar{i}} \mathbf{Z}_{\bar{i}}^\dagger \right\} \quad (2)$$

and

$$f_1(\mathbf{Z}_{\bar{i}}; \alpha, \mathbf{q}, \mathbf{M}) = \frac{1}{[\pi^N \det(\mathbf{M} + \mathbf{q}\mathbf{q}^\dagger)]^H} \times \text{etr} \left\{ -(\mathbf{M} + \mathbf{q}\mathbf{q}^\dagger)^{-1} \mathbf{Z}_{\alpha, \bar{i}} \mathbf{Z}_{\alpha, \bar{i}}^\dagger \right\}, \quad (3)$$

respectively, whereas the PDF of $\mathbf{R} = [\mathbf{r}_1 \dots \mathbf{r}_K]$ under both hypotheses has the following expression

$$f(\mathbf{R}; \mathbf{M}) = \frac{1}{[\pi^N \det(\mathbf{M})]^K} \text{etr} \left\{ -\mathbf{M}^{-1} \mathbf{R} \mathbf{R}^\dagger \right\}. \quad (4)$$

Finally, let us define the likelihood function of the unknown parameters under \mathcal{H}_i , $i = 0, 1$, as

$$\mathcal{L}_0(\mathbf{q}, \mathbf{M}) = f_0(\mathbf{Z}_{\bar{i}}; \mathbf{q}, \mathbf{M}), \quad (5)$$

$$\mathcal{L}_1(\alpha, \mathbf{q}, \mathbf{M}) = f_1(\mathbf{Z}_{\bar{i}}; \alpha, \mathbf{q}, \mathbf{M}). \quad (6)$$

Now, we formulate the detection problem from another perspective. Specifically, observe that the radar system, at each dwell, collects a realization of the NCP. Thus, it is reasonable to compare (1) with another detection problem formulated as

$$\begin{cases} \mathcal{H}_0 : \begin{cases} \mathbf{z}_{\bar{i}} \sim \mathcal{CN}_N(\beta\mathbf{q}, \mathbf{M}), \\ \mathbf{z}_i \sim \mathcal{CN}_N(\beta_i\mathbf{q}, \mathbf{M}), & i \in \Omega \setminus \{\bar{i}\}, \\ \mathbf{r}_k \sim \mathcal{CN}_N(\mathbf{0}, \mathbf{M}), & k = 1, \dots, K, \end{cases} \\ \mathcal{H}_1 : \begin{cases} \mathbf{z}_{\bar{i}} \sim \mathcal{CN}_N(\alpha\mathbf{v} + \beta\mathbf{q}, \mathbf{M}), \\ \mathbf{z}_i \sim \mathcal{CN}_N(\beta_i\mathbf{q}, \mathbf{M}), & i \in \Omega \setminus \{\bar{i}\}, \\ \mathbf{r}_k \sim \mathcal{CN}_N(\mathbf{0}, \mathbf{M}), & k = 1, \dots, K, \end{cases} \end{cases} \quad (7)$$

where

- $\beta \in \mathbb{C}$ and $\beta_i \in \mathbb{C}$ are unknown deterministic factors representative of the different jammer amplitudes;
- $\mathbf{q} \in \mathbb{C}^{N \times 1}$ is an unknown deterministic vector representing the contribution of the NCP jamming.

¹Note that the steering corresponds to a ULA with half-wavelength spacing.

Again, we have that

- $\alpha \in \mathbb{C}$ is an unknown deterministic factor accounting for target response and channel effects;
- $\mathbf{v} \in \mathbb{C}^{N \times 1}$ is the known steering vector of the target;
- $\mathbf{M} \in \mathbb{C}^{N \times N}$ is the unknown positive definite covariance matrix of thermal noise plus clutter.

Furthermore, in this case, the PDF of $\mathbf{Z}_{\bar{i}}$, under \mathcal{H}_l , $l = 0, 1$, exhibits the following expression

$$f(\mathbf{z}_{\bar{i}}, \mathbf{Z}_{\Omega, \bar{i}}; l\alpha, \beta, \beta_i, i \in \Omega \setminus \{\bar{i}\}, \mathbf{M}, \mathbf{q}) = \frac{1}{[\pi^N \det(\mathbf{M})]^H} \exp \left\{ -\text{Tr} \left[\mathbf{M}^{-1} \left((\mathbf{z}_{\bar{i}} - l\alpha\mathbf{v} - \beta\mathbf{q})(\mathbf{z}_{\bar{i}} - l\alpha\mathbf{v} - \beta\mathbf{q})^\dagger + \sum_{i \in \Omega \setminus \{\bar{i}\}} (\mathbf{z}_i - \beta_i\mathbf{q})(\mathbf{z}_i - \beta_i\mathbf{q})^\dagger \right) \right] \right\}, \quad (8)$$

while the likelihood functions under \mathcal{H}_l , $l = 0, 1$, are given by

$$\begin{aligned} \mathcal{L}_0(\beta, \beta_i, i \in \Omega \setminus \{\bar{i}\}, \mathbf{M}, \mathbf{q}) &= f(\mathbf{z}_{\bar{i}}, \mathbf{Z}_{\Omega, \bar{i}}; 0, \beta, \beta_i, i \in \Omega \setminus \{\bar{i}\}, \mathbf{M}, \mathbf{q}), \\ \mathcal{L}_1(\alpha, \beta, \beta_i, i \in \Omega \setminus \{\bar{i}\}, \mathbf{M}, \mathbf{q}) &= f(\mathbf{z}_{\bar{i}}, \mathbf{Z}_{\Omega, \bar{i}}; \alpha, \beta, \beta_i, i \in \Omega \setminus \{\bar{i}\}, \mathbf{M}, \mathbf{q}). \end{aligned} \quad (9)$$

III. DETECTOR DESIGNS

In this section, we devise adaptive decision schemes for problems (1) and (7). To this end, observe that we cannot apply the Neyman-Pearson criterion since parameters α , β , β_i , \mathbf{M} and \mathbf{q} are not known. For this reason, we have to resort to ad hoc solutions. In particular, we adopt the two-step GLRT-based design procedure: first we derive the GLRT for known \mathbf{M} ; then we obtain an adaptive detector replacing the unknown matrix \mathbf{M} with an estimate based on secondary data. Thus, the main problem to solve is to discriminate between the interference-only-hypothesis \mathcal{H}_0 and the signal-plus-interference-hypothesis \mathcal{H}_1 based on $\mathbf{z}_{\bar{i}}$ and $\mathbf{Z}_{\Omega, \bar{i}}$ only (for known \mathbf{M}).

A. An Adaptive Architecture for Problem (1)

The GLRT for known \mathbf{M} is given by

$$\frac{\max_{\alpha, \mathbf{q}} \mathcal{L}_1(\alpha, \mathbf{q}, \mathbf{M})}{\max_{\mathbf{q}} \mathcal{L}_0(\mathbf{q}, \mathbf{M})} \underset{\mathcal{H}_0}{\overset{\mathcal{H}_1}{\geq}} \eta, \quad (10)$$

where η is the threshold² to be set according to the desired value of the probability of false alarm (P_{fa}).

Maximization of the PDF under \mathcal{H}_0 can be conducted using the following identities

$$\begin{aligned} \det(\mathbf{M} + \mathbf{q}\mathbf{q}^\dagger) &= \det(\mathbf{M}) \det(\mathbf{I}_N + \mathbf{M}^{-1/2} \mathbf{q}\mathbf{q}^\dagger \mathbf{M}^{-1/2}) \\ &= \det(\mathbf{M}) (1 + \mathbf{u}^\dagger \mathbf{u}), \end{aligned} \quad (11)$$

²Hereafter, η denotes any modification of the original threshold.

where $\mathbf{u} = \mathbf{M}^{-1/2} \mathbf{q}$ and

$$\begin{aligned} &\text{Tr} \left[(\mathbf{M} + \mathbf{q}\mathbf{q}^\dagger)^{-1} \mathbf{Z}_{\bar{i}} \mathbf{Z}_{\bar{i}}^\dagger \right] \\ &= \text{Tr} \left[\mathbf{M}^{-1/2} (\mathbf{I}_N + \mathbf{u}\mathbf{u}^\dagger)^{-1} \mathbf{X}_{\bar{i}} \mathbf{Z}_{\bar{i}}^\dagger \right] \\ &= \text{Tr} \left[(\mathbf{I}_N + \mathbf{u}\mathbf{u}^\dagger)^{-1} \mathbf{X}_{\bar{i}} \mathbf{X}_{\bar{i}}^\dagger \right] \\ &= \text{Tr} \left[\mathbf{X}_{\bar{i}} \mathbf{X}_{\bar{i}}^\dagger - \frac{\mathbf{u}\mathbf{u}^\dagger}{1 + \mathbf{u}^\dagger \mathbf{u}} \mathbf{X}_{\bar{i}} \mathbf{X}_{\bar{i}}^\dagger \right] \end{aligned} \quad (12)$$

where the last equality in equation (12) is obtained using the matrix inversion lemma while $\mathbf{X}_{\bar{i}} = \mathbf{M}^{-1/2} \mathbf{Z}_{\bar{i}} = \mathbf{M}^{-1/2} [\mathbf{z}_{\bar{i}} \ \mathbf{Z}_{\Omega, \bar{i}}] = [\mathbf{x}_{\bar{i}} \ \mathbf{X}_{\Omega, \bar{i}}]$. Maximization under the \mathcal{H}_1 hypothesis is conducted using identity (11), but replacing (12) with

$$\begin{aligned} &\text{Tr} \left[(\mathbf{M} + \mathbf{q}\mathbf{q}^\dagger)^{-1} \mathbf{Z}_{\alpha, \bar{i}} \mathbf{Z}_{\alpha, \bar{i}}^\dagger \right] \\ &= \text{Tr} \left[\mathbf{X}_{\alpha, \bar{i}} \mathbf{X}_{\alpha, \bar{i}}^\dagger - \frac{\mathbf{u}\mathbf{u}^\dagger}{1 + \mathbf{u}^\dagger \mathbf{u}} \mathbf{X}_{\alpha, \bar{i}} \mathbf{X}_{\alpha, \bar{i}}^\dagger \right] \end{aligned}$$

where $\mathbf{X}_{\alpha, \bar{i}} = \mathbf{M}^{-1/2} \mathbf{Z}_{\alpha, \bar{i}} = [\mathbf{x}_{\alpha, \bar{i}} \ \mathbf{X}_{\Omega, \bar{i}}]$ and, in particular, $\mathbf{x}_{\alpha, \bar{i}} = \mathbf{M}^{-1/2} (\mathbf{z}_{\bar{i}} - \alpha\mathbf{v})$. It follows that the likelihood functions under \mathcal{H}_0 and \mathcal{H}_1 can be re-written as

$$\begin{aligned} \mathcal{L}_0(\mathbf{q}, \mathbf{M}) &= \frac{1}{[\pi^N \det(\mathbf{M}) (1 + \mathbf{u}^\dagger \mathbf{u})]^H} \\ &\times \text{etr} \left\{ -\mathbf{X}_{\bar{i}} \mathbf{X}_{\bar{i}}^\dagger + \frac{\mathbf{u}\mathbf{u}^\dagger}{1 + \mathbf{u}^\dagger \mathbf{u}} \mathbf{X}_{\bar{i}} \mathbf{X}_{\bar{i}}^\dagger \right\} \end{aligned} \quad (13)$$

and

$$\begin{aligned} \mathcal{L}_1(\alpha, \mathbf{q}, \mathbf{M}) &= \frac{1}{[\pi^N \det(\mathbf{M}) (1 + \mathbf{u}^\dagger \mathbf{u})]^H} \\ &\times \text{etr} \left\{ -\mathbf{X}_{\alpha, \bar{i}} \mathbf{X}_{\alpha, \bar{i}}^\dagger + \frac{\mathbf{u}\mathbf{u}^\dagger}{1 + \mathbf{u}^\dagger \mathbf{u}} \mathbf{X}_{\alpha, \bar{i}} \mathbf{X}_{\alpha, \bar{i}}^\dagger \right\}, \end{aligned} \quad (14)$$

respectively.

Now, we focus on the maximization of the PDF under \mathcal{H}_0 . To this end, observe that \mathbf{u} , borrowing the approach developed in [30], can be represented as $\mathbf{u} = \sqrt{p} \mathbf{u}_0$ with $p = \mathbf{u}^\dagger \mathbf{u} = \|\mathbf{u}\|^2 > 0$ and, hence, $\|\mathbf{u}_0\| = 1$. For future reference, we also define by \mathcal{S} the N -sphere centered at the origin with unit radius; thus, condition $\mathbf{u}_0^\dagger \mathbf{u}_0 = \|\mathbf{u}_0\|^2 = 1$ is equivalent to $\mathbf{u}_0 \in \mathcal{S}$.

It follows that

$$\begin{aligned} \max_{\mathbf{q}} \mathcal{L}_0(\mathbf{q}, \mathbf{M}) &= \frac{1}{[\pi^N \det(\mathbf{M})]^H} \text{etr} \left\{ -\mathbf{X}_{\bar{i}} \mathbf{X}_{\bar{i}}^\dagger \right\} \\ &\times \max_{\mathbf{u}_0, p} \frac{1}{(1+p)^H} \text{etr} \left\{ \frac{p \mathbf{u}_0 \mathbf{u}_0^\dagger}{1+p} \mathbf{X}_{\bar{i}} \mathbf{X}_{\bar{i}}^\dagger \right\}. \end{aligned}$$

Thus, for known \mathbf{u}_0 , maximizing \mathcal{L}_0 with respect to p is tantamount to maximizing

$$g(p) = \frac{1}{(1+p)^H} \exp \left\{ \frac{p}{1+p} \mathbf{u}_0^\dagger \mathbf{X}_{\bar{i}} \mathbf{X}_{\bar{i}}^\dagger \mathbf{u}_0 \right\} \quad (15)$$

with respect to $p \geq 0$. It can be shown that the maximum is attained at

$$\hat{p} = \begin{cases} \frac{\mathbf{u}_0^\dagger \mathbf{X}_{\bar{i}} \mathbf{X}_{\bar{i}}^\dagger \mathbf{u}_0}{H} - 1, & \text{if } \frac{\mathbf{u}_0^\dagger \mathbf{X}_{\bar{i}} \mathbf{X}_{\bar{i}}^\dagger \mathbf{u}_0}{H} > 1, \\ 0, & \text{otherwise,} \end{cases} \quad (16)$$

and is given by

$$\begin{aligned} & \max_{p \geq 0} g(p) \\ &= \begin{cases} \left[\frac{H}{\mathbf{u}_0^\dagger \mathbf{X}_{\bar{i}} \mathbf{X}_{\bar{i}}^\dagger \mathbf{u}_0} \right]^H \\ \quad \times \exp\{\mathbf{u}_0^\dagger \mathbf{X}_{\bar{i}} \mathbf{X}_{\bar{i}}^\dagger \mathbf{u}_0 - H\}, & \text{if } \frac{\mathbf{u}_0^\dagger \mathbf{X}_{\bar{i}} \mathbf{X}_{\bar{i}}^\dagger \mathbf{u}_0}{H} > 1, \\ 1, & \text{otherwise.} \end{cases} \end{aligned} \quad (17)$$

Now, we let

$$h(x) = \begin{cases} \left[\frac{H}{x} \right]^H e^{x-H}, & x \in (H, +\infty), \\ 1, & x \in [0, H], \end{cases}$$

and observe that it is a strictly increasing function of x over $[H, +\infty)$ (and constant over $[0, H]$). It follows that to maximize \mathcal{L}_0 with respect to \mathbf{u} it is sufficient to plug the maximizer of $\mathbf{u}_0^\dagger \mathbf{X}_{\bar{i}} \mathbf{X}_{\bar{i}}^\dagger \mathbf{u}_0$ with respect to \mathbf{u}_0 into $\max_{p \geq 0} g(p)$. Using the Rayleigh-Ritz theorem [31], we obtain

$$\max_{\mathbf{u}_0 \in \mathcal{S}} \mathbf{u}_0^\dagger \mathbf{X}_{\bar{i}} \mathbf{X}_{\bar{i}}^\dagger \mathbf{u}_0 = \lambda_1(\mathbf{X}_{\bar{i}} \mathbf{X}_{\bar{i}}^\dagger), \quad (18)$$

where $\lambda_1(\cdot)$ denotes the maximum eigenvalue of the matrix argument and a maximizer for \mathbf{u}_0 is a normalized eigenvector of the matrix $\mathbf{X}_{\bar{i}} \mathbf{X}_{\bar{i}}^\dagger$ corresponding to $\lambda_1(\mathbf{X}_{\bar{i}} \mathbf{X}_{\bar{i}}^\dagger)$. Thus, we can conclude that

$$\begin{aligned} \max_{\mathbf{q}} \mathcal{L}_0(\mathbf{q}, \mathbf{M}) &= \frac{1}{[\pi^N \det(\mathbf{M})]^H} \text{etr} \left\{ -\mathbf{X}_{\bar{i}} \mathbf{X}_{\bar{i}}^\dagger \right\} \\ &\times \begin{cases} \left[\frac{H}{\lambda_1(\mathbf{X}_{\bar{i}} \mathbf{X}_{\bar{i}}^\dagger)} \right]^H \\ \quad \times \exp \left\{ \lambda_1(\mathbf{X}_{\bar{i}} \mathbf{X}_{\bar{i}}^\dagger) - H \right\}, & \text{if } \frac{\lambda_1(\mathbf{X}_{\bar{i}} \mathbf{X}_{\bar{i}}^\dagger)}{H} > 1, \\ 1, & \text{otherwise.} \end{cases} \end{aligned} \quad (19)$$

As for the optimization problem under \mathcal{H}_1 , let us compute the logarithm of the likelihood function (14) neglecting the terms independent of α and \mathbf{u} to obtain

$$\begin{aligned} g(\alpha, p, \mathbf{u}_0) &= -H \log(1 + \mathbf{u}^\dagger \mathbf{u}) \\ &\quad - \text{Tr} \left[\left(\mathbf{I}_N - \frac{\mathbf{u} \mathbf{u}^\dagger}{1 + \mathbf{u}^\dagger \mathbf{u}} \right) \mathbf{S}_{\Omega, \bar{i}} \right] \\ &\quad - \text{Tr} \left[\left(\mathbf{I}_N - \frac{\mathbf{u} \mathbf{u}^\dagger}{1 + \mathbf{u}^\dagger \mathbf{u}} \right) \mathbf{S}_{\alpha, \bar{i}} \right] \end{aligned}$$

$$\begin{aligned} &= -H \log(1 + \mathbf{u}^\dagger \mathbf{u}) + \frac{\mathbf{u}^\dagger \mathbf{S}_{\Omega, \bar{i}} \mathbf{u}}{1 + \mathbf{u}^\dagger \mathbf{u}} \\ &\quad + \frac{|\mathbf{x}_{\alpha, \bar{i}}^\dagger \mathbf{u}|^2}{1 + \mathbf{u}^\dagger \mathbf{u}} - \mathbf{x}_{\alpha, \bar{i}}^\dagger \mathbf{x}_{\alpha, \bar{i}} - \text{Tr} [\mathbf{S}_{\Omega, \bar{i}}] \\ &= -H \log(1 + p) + \frac{p}{1 + p} \mathbf{u}_0^\dagger \mathbf{S}_{\Omega, \bar{i}} \mathbf{u}_0 \\ &\quad + \frac{p}{1 + p} |\mathbf{x}_{\alpha, \bar{i}}^\dagger \mathbf{u}_0|^2 - \mathbf{x}_{\alpha, \bar{i}}^\dagger \mathbf{x}_{\alpha, \bar{i}} - \text{Tr} [\mathbf{S}_{\Omega, \bar{i}}], \end{aligned} \quad (20)$$

where $\mathbf{S}_{\Omega, \bar{i}} = \mathbf{X}_{\Omega, \bar{i}} \mathbf{X}_{\Omega, \bar{i}}^\dagger$ and $\mathbf{S}_{\alpha, \bar{i}} = \mathbf{x}_{\alpha, \bar{i}} \mathbf{x}_{\alpha, \bar{i}}^\dagger$.

It follows that maximizing $\mathcal{L}_1(\alpha, \mathbf{q}, \mathbf{M})$ with respect to α and \mathbf{q} is tantamount to

$$\max_{\alpha, p, \mathbf{u}_0} g(\alpha, p, \mathbf{u}_0). \quad (21)$$

However, this joint maximization with respect to α , p , and \mathbf{u}_0 is not an analytically tractable problem at least to the best of authors' knowledge³. For this reason, we resort to a suboptimum approach relying on alternating maximization [27]–[29]. Specifically, let us assume that $\mathbf{u}_0 = \mathbf{u}_0^{(n)}$ and $p = p^{(n)}$ are known, then it is not difficult to show that

$$\begin{aligned} \alpha^{(n)} &= \arg \max_{\alpha} g(\alpha, p^{(n)}, \mathbf{u}_0^{(n)}) \\ &= \arg \min_{\alpha} \mathbf{x}_{\alpha, \bar{i}}^\dagger \left[\mathbf{I}_N - \frac{p^{(n)}}{1 + p^{(n)}} \mathbf{u}_0^{(n)} (\mathbf{u}_0^{(n)})^\dagger \right] \mathbf{x}_{\alpha, \bar{i}} \\ &= \frac{\mathbf{v}_0^\dagger \left[\mathbf{I}_N - \frac{p^{(n)}}{1 + p^{(n)}} \mathbf{u}_0^{(n)} (\mathbf{u}_0^{(n)})^\dagger \right] \mathbf{x}_{\bar{i}}}{\mathbf{v}_0^\dagger \left[\mathbf{I}_N - \frac{p^{(n)}}{1 + p^{(n)}} \mathbf{u}_0^{(n)} (\mathbf{u}_0^{(n)})^\dagger \right] \mathbf{v}_0}, \end{aligned} \quad (22)$$

where $\mathbf{v}_0 = \mathbf{M}^{-1/2} \mathbf{v}$. Now, let us exploit $\alpha^{(n)}$ to estimate \mathbf{u}_0 and p , namely to solve the problem

$$\max_{p, \mathbf{u}_0 \in \mathcal{S}} g(\alpha^{(n)}, p, \mathbf{u}_0). \quad (23)$$

To this end, following the same line of reasoning as for \mathcal{H}_0 , we obtain that

$$\begin{aligned} \left[\begin{matrix} p^{(n+1)} \\ \mathbf{u}_0^{(n+1)} \end{matrix} \right] &= \arg \max_{p, \mathbf{u}_0 \in \mathcal{S}} g(\alpha^{(n)}, p, \mathbf{u}_0) \\ &= \left[\max \{ \lambda_1(\mathbf{S}_{\Omega, \bar{i}} + \mathbf{x}_{\alpha^{(n)}, \bar{i}} \mathbf{x}_{\alpha^{(n)}, \bar{i}}^\dagger) / H - 1, 0 \} \right], \\ &\quad \mathbf{b}_1 \end{aligned} \quad (24)$$

where we remember that $\lambda_1(\cdot)$ is the maximum eigenvalue of the matrix argument, $\mathbf{x}_{\alpha^{(n)}, \bar{i}}$ is obtained replacing α with $\alpha^{(n)}$ in $\mathbf{x}_{\alpha, \bar{i}}$, and \mathbf{b}_1 is a normalized eigenvector corresponding to $\lambda_1(\mathbf{S}_{\Omega, \bar{i}} + \mathbf{x}_{\alpha^{(n)}, \bar{i}} \mathbf{x}_{\alpha^{(n)}, \bar{i}}^\dagger)$.

³As a matter of fact, applying the classical maximum likelihood approach to $g(\alpha, p, \mathbf{u}_0)$ leads to difficult equations regardless the parameter optimization order as it stems from the expressions of the iterative parameter estimates given below.

Iterating the above estimation procedure, we come up with the following nondecreasing sequence

$$\begin{aligned} \mathcal{L}_1(\alpha^{(0)}, \mathbf{q}^{(0)}, \mathbf{M}) &\leq \mathcal{L}_1(\alpha^{(0)}, \mathbf{q}^{(1)}, \mathbf{M}) \\ &\leq \mathcal{L}_1(\alpha^{(1)}, \mathbf{q}^{(1)}, \mathbf{M}) \leq \dots \leq \mathcal{L}_1(\alpha^{(n)}, \mathbf{q}^{(n)}, \mathbf{M}), \end{aligned} \quad (25)$$

where we start using for $\mathbf{q}^{(0)}$ a normalized steering vector from a sidelobe direction and $\mathbf{q}^{(i)} = p^{(i)} \mathbf{M}^{1/2} \mathbf{u}_0^{(i)}$, $i = 1, \dots, n$. Since the likelihood under \mathcal{H}_1 is bounded from the above with respect to α, p, \mathbf{u}_0 , the nondecreasing sequence (25) converges as n diverges and, hence, a suitable stopping criterion can be defined. For example, a possible strategy might consist in continuing the procedure until

$$\|\mathbf{q}^{(n)} - \mathbf{q}^{(n-1)}\| < \epsilon_q \quad \text{and/or} \quad |\alpha^{(n)} - \alpha^{(n-1)}| < \epsilon_\alpha. \quad (26)$$

Another approach might be that the alternating procedure terminates when $n > N_{max}$ with N_{max} the maximum allowable number of iterations. We will use the latter stopping criterion with N_{max} chosen in the next section.

To prove that the likelihood is bounded from the above, we re-write g as the sum of three (bounded above) functions, namely as

$$\begin{aligned} g(\alpha, p, \mathbf{u}_0) &= -H \log(1+p) - \text{Tr} [\mathbf{S}_{\Omega, \bar{i}}] + \frac{p}{1+p} \mathbf{u}_0^\dagger \mathbf{S}_{\Omega, \bar{i}} \mathbf{u}_0 \\ &\quad + \frac{p}{1+p} |\mathbf{x}_{\alpha, \bar{i}}^\dagger \mathbf{u}_0|^2 - \mathbf{x}_{\alpha, \bar{i}}^\dagger \mathbf{x}_{\alpha, \bar{i}} \\ &= g_1(p) + g_2(p, \mathbf{u}_0) + g_3(\alpha, p, \mathbf{u}_0) \end{aligned} \quad (27)$$

with

$$g_1(p) = -H \log(1+p) - \text{Tr} [\mathbf{S}_{\Omega, \bar{i}}], \quad (28)$$

$$g_2(p, \mathbf{u}_0) = \frac{p}{1+p} \mathbf{u}_0^\dagger \mathbf{S}_{\Omega, \bar{i}} \mathbf{u}_0, \quad (29)$$

$$g_3(\alpha, p, \mathbf{u}_0) = \frac{p}{1+p} |\mathbf{x}_{\alpha, \bar{i}}^\dagger \mathbf{u}_0|^2 - \mathbf{x}_{\alpha, \bar{i}}^\dagger \mathbf{x}_{\alpha, \bar{i}}. \quad (30)$$

Then, it is sufficient to observe that

- $g_1(p) \leq 0, \forall p \geq 0$;
- $\forall p \geq 0, \mathbf{u}_0 \in \mathcal{S}$ the second term $g_2(p, \mathbf{u}_0)$ can be trivially upperbounded as

$$\begin{aligned} g_2(p, \mathbf{u}_0) &= \frac{p}{1+p} \mathbf{u}_0^\dagger \mathbf{S}_{\Omega, \bar{i}} \mathbf{u}_0 \\ &\leq \mathbf{u}_0^\dagger \mathbf{S}_{\Omega, \bar{i}} \mathbf{u}_0 (\leq \lambda_1(\mathbf{S}_{\Omega, \bar{i}})) \end{aligned} \quad (31)$$

and the right-most hand side attains a maximum since it is a continuous function of \mathbf{u}_0 over a compact set (\mathbf{u}_0 belongs to the N -sphere with unit radius);

- the third term can be re-written as

$$g_3(\alpha, p, \mathbf{u}_0) = -\mathbf{x}_{\alpha, \bar{i}}^\dagger \left(\mathbf{I}_N - \frac{p}{1+p} \mathbf{u}_0 \mathbf{u}_0^\dagger \right) \mathbf{x}_{\alpha, \bar{i}};$$

since the matrix $\mathbf{I}_N - \frac{p}{1+p} \mathbf{u}_0 \mathbf{u}_0^\dagger$ is positive definite $\forall p \geq 0$ and $\mathbf{u}_0 \in \mathcal{S}$, it follows that $g_3(\alpha, p, \mathbf{u}_0) \leq 0, \forall \alpha \in \mathbb{C}, p \geq 0, \mathbf{u}_0 \in \mathcal{S}$.

Finally, \mathbf{M} can be estimated using secondary data \mathbf{R} as

$$\widehat{\mathbf{M}} = \frac{1}{K} \mathbf{R} \mathbf{R}^\dagger. \quad (32)$$

Algorithm 1: Procedure to compute the decision statistic of R-NCP-D.

Input: $\mathbf{z}_{\bar{i}}, \mathbf{Z}_{\Omega, \bar{i}}, \mathbf{R}, \mathbf{u}_0^{(0)}, p^{(0)}, \mathbf{v}$

Output: Decision statistic of R-NCP-D

- 1: Compute $\widehat{\mathbf{M}} = \frac{1}{K} \mathbf{R} \mathbf{R}^\dagger$
 - 2: Compute $\widehat{\mathbf{X}}_{\bar{i}} = \widehat{\mathbf{M}}^{-1/2} [\mathbf{z}_{\bar{i}}, \mathbf{Z}_{\Omega, \bar{i}}], \lambda_1(\widehat{\mathbf{X}}_{\bar{i}} \widehat{\mathbf{X}}_{\bar{i}}^\dagger)$, and $\widehat{\mathbf{v}}_0 = \widehat{\mathbf{M}}^{-1/2} \mathbf{v}$
 - 3: Compute (19) with $\widehat{\mathbf{X}}_{\bar{i}}$ and $\widehat{\mathbf{M}}$ in place of $\mathbf{X}_{\bar{i}}$ and \mathbf{M} , respectively, and denote the result by $\tilde{\mathcal{L}}_0$
 - 4: Set $n = 0$
 - 5: Compute $\alpha^{(n)}$ using (22) with $\widehat{\mathbf{X}}_{\bar{i}}$ and $\widehat{\mathbf{v}}_0$ in place of $\mathbf{X}_{\bar{i}}$ and \mathbf{v}_0 , respectively
 - 6: If $n < N_{max}$ go to step 7 else go to step 9
 - 7: Compute $p^{(n+1)}$ and $\mathbf{u}_0^{(n+1)}$ using (24) with $\widehat{\mathbf{X}}_{\bar{i}}$ and $\widehat{\mathbf{v}}_0$ in place of $\mathbf{X}_{\bar{i}}$ and \mathbf{v}_0 , respectively
 - 8: Set $n = n + 1$ and go to step 5
 - 9: Return $\mathcal{L}_1(\alpha^{(n)}, p^{(n)}, \mathbf{u}_0^{(n)}, \widehat{\mathbf{M}}) / \tilde{\mathcal{L}}_0$
-

This decision scheme is referred to in the following as random NCP detector (R-NCP-D). The steps to compute the decision statistic of R-NCP-D are summarized in Algorithm 1.

B. An Adaptive Architecture for Problem (7)

In this case, the GLRT for known \mathbf{M} is given by

$$\frac{\max_{\alpha, \beta, \beta_i, i \in \Omega \setminus \{\bar{i}\}, \mathbf{q}} \mathcal{L}_1(\alpha, \beta, \beta_i, i \in \Omega \setminus \{\bar{i}\}, \mathbf{M}, \mathbf{q})}{\max_{\beta, \beta_i, i \in \Omega \setminus \{\bar{i}\}, \mathbf{q}} \mathcal{L}_0(\beta, \beta_i, i \in \Omega \setminus \{\bar{i}\}, \mathbf{M}, \mathbf{q})} \underset{\mathcal{H}_0}{\overset{\mathcal{H}_1}{\geq}} \eta. \quad (33)$$

Focusing on the maximization of the PDF under \mathcal{H}_0 , we observe that maximizing \mathcal{L}_0 is tantamount to maximizing⁴

$$\begin{aligned} &v(\beta, \beta_i, i \in \Omega \setminus \{\bar{i}\}, \mathbf{q}) \\ &= \text{etr} \left\{ -\mathbf{M}^{-1} \left[(\mathbf{z}_{\bar{i}} - \beta \mathbf{q})(\mathbf{z}_{\bar{i}} - \beta \mathbf{q})^\dagger \right. \right. \\ &\quad \left. \left. + \sum_{i \in \Omega \setminus \{\bar{i}\}} (\mathbf{z}_i - \beta_i \mathbf{q})(\mathbf{z}_i - \beta_i \mathbf{q})^\dagger \right] \right\} \end{aligned} \quad (34)$$

Furthermore, it can be proved that

$$\begin{aligned} &\min_{\beta} (\mathbf{z}_{\bar{i}} - \beta \mathbf{q})^\dagger \mathbf{M}^{-1} (\mathbf{z}_{\bar{i}} - \beta \mathbf{q}) \\ &= \mathbf{z}_{\bar{i}}^\dagger \mathbf{M}^{-1} \mathbf{z}_{\bar{i}} - \frac{\mathbf{z}_{\bar{i}}^\dagger \mathbf{M}^{-1} \mathbf{q} \mathbf{q}^\dagger \mathbf{M}^{-1} \mathbf{z}_{\bar{i}}}{\mathbf{q}^\dagger \mathbf{M}^{-1} \mathbf{q}} \end{aligned} \quad (35)$$

and

$$\begin{aligned} &\min_{\beta_i} \sum_{i \in \Omega \setminus \{\bar{i}\}} (\mathbf{z}_i - \beta_i \mathbf{q})^\dagger \mathbf{M}^{-1} (\mathbf{z}_i - \beta_i \mathbf{q}) \\ &= \sum_{i \in \Omega \setminus \{\bar{i}\}} \left(\mathbf{z}_i^\dagger \mathbf{M}^{-1} \mathbf{z}_i - \frac{\mathbf{z}_i^\dagger \mathbf{M}^{-1} \mathbf{q} \mathbf{q}^\dagger \mathbf{M}^{-1} \mathbf{z}_i}{\mathbf{q}^\dagger \mathbf{M}^{-1} \mathbf{q}} \right). \end{aligned} \quad (36)$$

⁴Note that this optimization is a special case of one of the instances considered in [23].

Thus, the maximization of w with respect to β and β_i leads to

$$\begin{aligned}
& \max_{\beta, \beta_i, i \in \Omega \setminus \{\bar{i}\}, \mathbf{q}} w(\beta, \beta_i, i \in \Omega \setminus \{\bar{i}\}, \mathbf{q}) \\
&= \max_{\mathbf{q}} \exp \left[\frac{\mathbf{z}_{\bar{i}}^\dagger \mathbf{M}^{-1} \mathbf{q} \mathbf{q}^\dagger \mathbf{M}^{-1} \mathbf{z}_{\bar{i}}}{\mathbf{q}^\dagger \mathbf{M}^{-1} \mathbf{q}} - \mathbf{z}_{\bar{i}}^\dagger \mathbf{M}^{-1} \mathbf{z}_{\bar{i}} \right] \\
&+ \sum_{i \in \Omega \setminus \{\bar{i}\}} \left(\frac{\mathbf{z}_i^\dagger \mathbf{M}^{-1} \mathbf{q} \mathbf{q}^\dagger \mathbf{M}^{-1} \mathbf{z}_i}{\mathbf{q}^\dagger \mathbf{M}^{-1} \mathbf{q}} - \mathbf{z}_i^\dagger \mathbf{M}^{-1} \mathbf{z}_i \right) \\
&= \max_{\mathbf{q}} \exp \left\{ \frac{\mathbf{q}^\dagger \mathbf{M}^{-1} \left[\mathbf{z}_{\bar{i}} \mathbf{z}_{\bar{i}}^\dagger + \sum_{i \in \Omega \setminus \{\bar{i}\}} \mathbf{z}_i \mathbf{z}_i^\dagger \right] \mathbf{M}^{-1} \mathbf{q}}{\mathbf{q}^\dagger \mathbf{M}^{-1} \mathbf{q}} \right. \\
&- \left. \left(\mathbf{z}_{\bar{i}}^\dagger \mathbf{M}^{-1} \mathbf{z}_{\bar{i}} + \sum_{i \in \Omega \setminus \{\bar{i}\}} \mathbf{z}_i^\dagger \mathbf{M}^{-1} \mathbf{z}_i \right) \right\} \\
&= \max_{\mathbf{u}} \exp \left\{ \frac{\mathbf{u}^\dagger \left[\mathbf{x}_{\bar{i}} \mathbf{x}_{\bar{i}}^\dagger + \sum_{i \in \Omega \setminus \{\bar{i}\}} \mathbf{x}_i \mathbf{x}_i^\dagger \right] \mathbf{u}}{\mathbf{u}^\dagger \mathbf{u}} \right. \\
&- \left. \left(\mathbf{x}_{\bar{i}}^\dagger \mathbf{x}_{\bar{i}} + \sum_{i \in \Omega \setminus \{\bar{i}\}} \mathbf{x}_i^\dagger \mathbf{x}_i \right) \right\} \\
&= \exp \{ \lambda_1(\mathbf{S}_1) - \text{Tr}(\mathbf{S}_1) \} \tag{37}
\end{aligned}$$

where $\mathbf{S}_1 = \mathbf{x}_{\bar{i}} \mathbf{x}_{\bar{i}}^\dagger + \sum_{i \in \Omega \setminus \{\bar{i}\}} \mathbf{x}_i \mathbf{x}_i^\dagger$ and we used the Rayleigh-Ritz theorem [31]. We also recall that $\mathbf{x}_i = \mathbf{M}^{-1/2} \mathbf{z}_i$ and $\mathbf{u} = \mathbf{M}^{-1/2} \mathbf{q}$.

Thus, we conclude that the compressed likelihood under \mathcal{H}_0 is given by

$$\begin{aligned}
& \max_{\beta, \beta_i, i \in \Omega \setminus \{\bar{i}\}, \mathbf{q}} \mathcal{L}_0(\beta, \beta_i, i \in \Omega \setminus \{\bar{i}\}, \mathbf{M}, \mathbf{q}) \\
&= \frac{1}{[\pi^N \det(\mathbf{M})]^H} \exp \{ \lambda_1(\mathbf{S}_1) - \text{Tr}(\mathbf{S}_1) \}. \tag{38}
\end{aligned}$$

As far as the maximization of the likelihood function under \mathcal{H}_1 is concerned, we first focus on α and observe that

$$\begin{aligned}
& \min_{\alpha} \left((\mathbf{z}_{\bar{i}} - \alpha \mathbf{v} - \beta \mathbf{q})^\dagger \mathbf{M}^{-1} (\mathbf{z}_{\bar{i}} - \alpha \mathbf{v} - \beta \mathbf{q}) \right) \\
&= (\mathbf{z}_{\bar{i}} - \beta \mathbf{q})^\dagger \mathbf{M}^{-1} (\mathbf{z}_{\bar{i}} - \beta \mathbf{q}) \\
&- \frac{(\mathbf{z}_{\bar{i}} - \beta \mathbf{q})^\dagger \mathbf{M}^{-1} \mathbf{v} \mathbf{v}^\dagger \mathbf{M}^{-1} (\mathbf{z}_{\bar{i}} - \beta \mathbf{q})}{\mathbf{v}^\dagger \mathbf{M}^{-1} \mathbf{v}}. \tag{39}
\end{aligned}$$

Thus, it turns out that

$$\begin{aligned}
& \max_{\alpha} \mathcal{L}_1(\alpha, \beta, \beta_i, i \in \Omega \setminus \{\bar{i}\}, \mathbf{M}, \mathbf{q}) = \frac{1}{[\pi^N \det(\mathbf{M})]^H} \\
&\times \exp \left\{ \frac{(\mathbf{z}_{\bar{i}} - \beta \mathbf{q})^\dagger \mathbf{M}^{-1} \mathbf{v} \mathbf{v}^\dagger \mathbf{M}^{-1} (\mathbf{z}_{\bar{i}} - \beta \mathbf{q})}{\mathbf{v}^\dagger \mathbf{M}^{-1} \mathbf{v}} \right. \\
&- (\mathbf{z}_{\bar{i}} - \beta \mathbf{q})^\dagger \mathbf{M}^{-1} (\mathbf{z}_{\bar{i}} - \beta \mathbf{q}) \\
&- \left. \sum_{i \in \Omega \setminus \{\bar{i}\}} (\mathbf{z}_i - \beta_i \mathbf{q})^\dagger \mathbf{M}^{-1} (\mathbf{z}_i - \beta_i \mathbf{q}) \right\}. \tag{40}
\end{aligned}$$

To the best of authors' knowledge, the maximization of (40) with respect to the remaining parameters cannot be conducted in closed form; in particular, maximizing with respect to \mathbf{u} first makes the resulting function of β and β_i difficult to optimize due to the fact that it contains matrix-valued functions of the parameters. For this reason, we exploit another alternating optimization procedure. To this end, we first re-write the partially-compressed likelihood as

$$\begin{aligned}
& \max_{\alpha} \mathcal{L}_1(\alpha, \beta, \beta_i, i \in \Omega \setminus \{\bar{i}\}, \mathbf{M}, \mathbf{q}) \\
&= \frac{1}{[\pi^N \det(\mathbf{M})]^H} \exp [-h(\mathbf{u}, \beta, \beta_i, i \in \Omega \setminus \{\bar{i}\})] \tag{41}
\end{aligned}$$

with

$$\begin{aligned}
h(\mathbf{u}, \beta, \beta_i, i \in \Omega \setminus \{\bar{i}\}) &= (\mathbf{x}_{\bar{i}} - \beta \mathbf{u})^\dagger \mathbf{P}_{\mathbf{v}_0}^\perp (\mathbf{x}_{\bar{i}} - \beta \mathbf{u}) \\
&+ \sum_{i \in \Omega \setminus \{\bar{i}\}} (\mathbf{x}_i - \beta_i \mathbf{u})^\dagger (\mathbf{x}_i - \beta_i \mathbf{u}) \tag{42}
\end{aligned}$$

where

$$\mathbf{P}_{\mathbf{v}_0}^\perp = \mathbf{I}_N - \frac{\mathbf{v}_0 \mathbf{v}_0^\dagger}{\mathbf{v}_0^\dagger \mathbf{v}_0}, \tag{43}$$

and, for the reader ease, we recall that $\mathbf{u} = \mathbf{M}^{-1/2} \mathbf{q}$, $\mathbf{x}_i = \mathbf{M}^{-1/2} \mathbf{z}_i$, $\mathbf{x}_{\bar{i}} = \mathbf{M}^{-1/2} \mathbf{z}_{\bar{i}}$, and $\mathbf{v}_0 = \mathbf{M}^{-1/2} \mathbf{v}$.

Then, assuming that $\beta = \beta^{(n)}$ and $\beta_i = \beta_i^{(n)}$ are given, we can focus on the maximization with respect to \mathbf{q} . To this end, setting to zero the first derivative⁵ of

$$h(\mathbf{u}, \beta^{(n)}, \beta_i^{(n)}, i \in \Omega \setminus \{\bar{i}\})$$

with respect to \mathbf{u} leads to

$$\begin{aligned}
& -\beta^{(n)*} \mathbf{P}_{\mathbf{v}_0}^\perp \mathbf{x}_{\bar{i}} + \left| \beta^{(n)} \right|^2 \mathbf{P}_{\mathbf{v}_0}^\perp \mathbf{u} \\
&- \sum_{i \in \Omega \setminus \{\bar{i}\}} \beta_i^{(n)*} \mathbf{x}_i + \sum_{i \in \Omega \setminus \{\bar{i}\}} \left| \beta_i^{(n)} \right|^2 \mathbf{u} = 0; \tag{45}
\end{aligned}$$

then

$$\begin{aligned}
\mathbf{u}^{(n)} &= \arg \min_{\mathbf{u}} \left\{ h(\mathbf{u}, \beta^{(n)}, \beta_i^{(n)}, i \in \Omega \setminus \{\bar{i}\}) \right\} \\
&= \left(\left| \beta^{(n)} \right|^2 \mathbf{P}_{\mathbf{v}_0}^\perp + \sum_{i \in \Omega \setminus \{\bar{i}\}} \left| \beta_i^{(n)} \right|^2 \mathbf{I}_N \right)^{-1} \\
&\left(\beta^{(n)*} \mathbf{P}_{\mathbf{v}_0}^\perp \mathbf{x}_{\bar{i}} + \sum_{i \in \Omega \setminus \{\bar{i}\}} \beta_i^{(n)*} \mathbf{x}_i \right). \tag{46}
\end{aligned}$$

⁵We make use of the following definition for the derivative of a real function $f(\alpha)$ with respect to the complex argument $\alpha = \alpha_r + j\alpha_i$, $\alpha_r, \alpha_i \in \mathbb{R}$, [32]

$$\frac{\partial f(\alpha)}{\partial \alpha} = \frac{1}{2} \left[\frac{\partial f(\alpha)}{\partial \alpha_r} - j \frac{\partial f(\alpha)}{\partial \alpha_i} \right]. \tag{44}$$

Algorithm 2: Procedure to compute the decision statistic of D-NCP-D.

Input: $z_{\bar{i}}, \mathbf{Z}_{\Omega, \bar{i}}, \mathbf{R}, \mathbf{u}^{(0)}$

Output: Decision statistic of D-NCP-D

- 1: Compute $\widehat{\mathbf{M}} = \frac{1}{K} \mathbf{R} \mathbf{R}^\dagger$,
- 2: Compute $\widehat{\mathbf{x}}_{\bar{i}} = \widehat{\mathbf{M}}^{-1/2} z_{\bar{i}}, \widehat{\mathbf{X}}_{\Omega, \bar{i}} = \widehat{\mathbf{M}}^{-1/2} \mathbf{Z}_{\Omega, \bar{i}},$
 $\widehat{\mathbf{S}}_1 = \widehat{\mathbf{x}}_{\bar{i}} \widehat{\mathbf{x}}_{\bar{i}}^\dagger + \widehat{\mathbf{X}}_{\Omega, \bar{i}} \widehat{\mathbf{X}}_{\Omega, \bar{i}}^\dagger$
- 3: Compute (38) with $\widehat{\mathbf{S}}_1$ and $\widehat{\mathbf{M}}$ in place of \mathbf{S}_1 and \mathbf{M} , respectively, and denote the result with $\widehat{\mathcal{L}}_0$
- 4: Compute $\widehat{\mathbf{v}}_0 = \widehat{\mathbf{M}}^{-1/2} \mathbf{v}$ and $P_{\widehat{\mathbf{v}}_0}^\perp = \mathbf{I}_N - \frac{\widehat{\mathbf{v}}_0 \widehat{\mathbf{v}}_0^\dagger}{\widehat{\mathbf{v}}_0^\dagger \widehat{\mathbf{v}}_0}$
- 5: Set $n = 0$
- 6: Compute $\beta^{(n+1)}$ and $\beta_i^{(n+1)}, i \in \Omega \setminus \{\bar{i}\}$, using (47) with $\widehat{\mathbf{x}}_{\bar{i}}, \widehat{\mathbf{X}}_{\Omega, \bar{i}},$ and $\widehat{\mathbf{v}}_0$ in place of $\mathbf{x}_{\bar{i}}, \mathbf{X}_{\Omega, \bar{i}},$ and \mathbf{v}_0 , respectively
- 7: If $n < N_{max}$ go to step 8 else go to step 10
- 8: Compute $\mathbf{u}^{(n+1)}$ using (46) with $\widehat{\mathbf{x}}_{\bar{i}}, \widehat{\mathbf{X}}_{\Omega, \bar{i}},$ and $\widehat{\mathbf{v}}_0$ in place of $\mathbf{x}_{\bar{i}}, \mathbf{X}_{\Omega, \bar{i}},$ and \mathbf{v}_0 , respectively
- 9: Set $n = n + 1$ and go to step 6
- 10: Return

$$\frac{\exp \left[-h \left(\mathbf{u}^{(n)}, \beta^{(n)}, \beta_i^{(n)}, i \in \Omega \setminus \{\bar{i}\} \right) \right] \left[\pi^N \det(\widehat{\mathbf{M}}) \right]^{-H}}{\widehat{\mathcal{L}}_0}$$

On the other hand, we can estimate $\beta^{(n+1)}$ and $\beta_i^{(n+1)}$, given $\mathbf{u}^{(n)}$, exploiting a standard least-squares result, i.e.,

$$\begin{aligned} \begin{bmatrix} \beta^{(n+1)} \\ \beta_i^{(n+1)} \end{bmatrix} &= \arg \max_{\beta, \beta_i} \left\{ \exp \left[-h \left(\mathbf{u}^{(n)}, \beta, \beta_i, i \in \Omega \setminus \{\bar{i}\} \right) \right] \right\} \\ &= \begin{bmatrix} \frac{\mathbf{u}^{(n)\dagger} \mathbf{P}_{\mathbf{v}_0}^\perp \mathbf{x}_{\bar{i}}}{\mathbf{u}^{(n)\dagger} \mathbf{P}_{\mathbf{v}_0}^\perp \mathbf{u}^{(n)}} \\ \frac{\mathbf{u}^{(n)\dagger} \mathbf{x}_i}{\mathbf{u}^{(n)\dagger} \mathbf{u}^{(n)}} \end{bmatrix}. \end{aligned} \quad (47)$$

The iterative procedure starts by replacing $\mathbf{u}^{(0)}$ with a normalized steering vector from the sidelobes. Moreover, as for the R-NCP-D, we stop alternating after a preassigned number of iterations.

Finally, replacing \mathbf{M} with the sample covariance matrix based upon the secondary data, we come up with an adaptive detector referred to in the following as deterministic NCP detector (D-NCP-D). The operations required to form the decision statistic of D-NCP-D are summarized in Algorithm 2.

IV. PERFORMANCE ASSESSMENT

The aim of this section is to investigate the performance of the proposed algorithms in terms of probability of detection (P_d). To this end, we resort to standard Monte Carlo counting techniques by evaluating the thresholds to ensure a preassigned P_{fa} and the P_d curves over $100/P_{fa}$ and 1000 independent trials, respectively. Data are generated according to the model

TABLE I
SIMULATION PARAMETERS SETUP

Symbol	Value	Description
N	8,16	Number of antennas
H_1	10	Number of contaminated cells on the left of the CUT
H_2	10	Number of contaminated cells on the right of the CUT
CNR	20 dB	Clutter-to-Noise Ratio
JNR	30 dB	Jammer-to-Noise Ratio
θ_j	35°	Angle Of Arrival (AOA) of the NCP jammer
P_{fa}	10^{-5}	False Alarm probability
N_{MC}	10^3	Number of independent trials to evaluate the probability of detection P_d

defined in problem (1), where

$$\mathbf{M} = \sigma_n^2 \mathbf{I}_N + p_c \mathbf{M}_c. \quad (48)$$

In (48), $\sigma_n^2 \mathbf{I}_N$ represents the thermal noise component with power σ_n^2 while $p_c \mathbf{M}_c$ is the clutter component with p_c the clutter power and \mathbf{M}_c the structure of the clutter covariance matrix; the clutter-to-noise ratio (CNR) is thus given by $\text{CNR} = p_c / \sigma_n^2$.

In the following, we set $\sigma_n^2 = 1$, CNR = 20 dB, and $\mathbf{M}_c(i, j) = \rho^{|i-j|}$ with $\rho = 0.9$ (recall that $\mathbf{M}_c(i, j)$ is the (i, j) th entry of \mathbf{M}_c). We recall that the victim radar is equipped with a ULA. The target response is computed according to the signal-to-clutter-plus-noise ratio (SCNR), whose expression is

$$\text{SCNR} = |\alpha|^2 \mathbf{v}(0)^\dagger \mathbf{M}^{-1} \mathbf{v}(0). \quad (49)$$

As for the NCP, we assume that, when it is present, it enters the antenna array response of the victim radar from the sidelobes with a power p_j such that the jammer-to-noise ratio (JNR), defined as $\text{JNR} = p_j / \sigma_n^2$, is 30 dB. In order to select the amount of primary data, we consider system parameter values of practical interest, namely we assume that the radar system transmits a linear frequency modulated pulse of duration $3 \mu\text{s}$ and bandwidth 5 MHz. Now, since the sampling time at which the range bins are generated is $2 \cdot 10^{-7}$ s, then the uncompressed pulse covers 15 range bins. Using 5 additional guard cells, we set $H_1 = H_2 = 10$. For the reader ease, all the simulation parameters are summarized in Table I.

Finally, for comparison purposes, we also report the P_d curves of the subspace detector (SD) proposed in [23], the adaptive matched filter (AMF) [33], which raises from a suitable modification of the derivation contained in Subsection III-B, which consists in forcing the constraint $\mathbf{q}^\dagger \mathbf{M}^{-1} \mathbf{v} = 0$ as shown in the appendix⁶, the adaptive coherence estimator (ACE) [34], [35] (also known as adaptive normalized matched filter), and Kelly's GLRT [36]. It is also important to notice that in the presence of NCP attack, another (heuristic) competitor would consist in projecting data onto the orthogonal complement of the subspace spanned by the jammer steering vector and in exploiting transformed data to build up a decision statistic as the AMF. However, such architecture requires that an estimate of jammer

⁶Recall from Table I that the jammer is located at 35° with respect to the array normal, leading to $\cos(\theta_{jt}) = 0.07$ for $N = 8$ and $\cos(\theta_{jt}) = 0.03$ for $N = 16$, where θ_{jt} is the angle between target and jammer steering vectors in the whitened observation space.

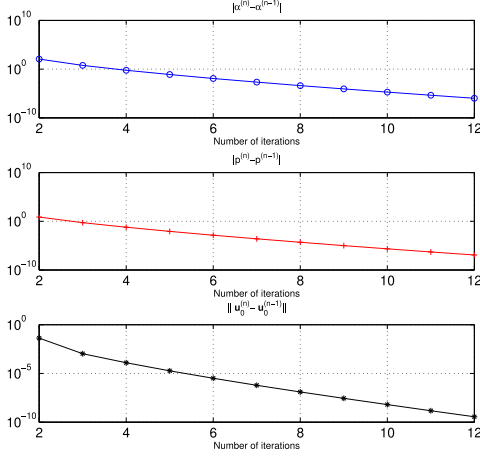


Fig. 3. Euclidean norm (or modulus) of the difference between the estimates at the n th iteration and those at the $(n - 1)$ th iteration versus the number of iterations for cyclic optimization of Subsection III-A.

AOA should be available. Now, due to the enormous amount of AOA estimation algorithms in the open literature, the choice of the “right” estimation procedure would be a critical issue affecting the detection performance. For this reason, we simplify the analysis assuming that jammer AOA is perfectly known and proceed by considering the following heuristic detector (HD)

$$\frac{\left| \mathbf{v}(\theta_j)^\dagger \mathbf{U}_j \left(\mathbf{U}_j^\dagger \widehat{\mathbf{M}} \mathbf{U}_j \right)^{-1} \mathbf{U}_j^\dagger \mathbf{z}_i \right|^2}{\mathbf{v}(\theta_j)^\dagger \mathbf{U}_j \left(\mathbf{U}_j^\dagger \widehat{\mathbf{M}} \mathbf{U}_j \right)^{-1} \mathbf{U}_j^\dagger \mathbf{v}(\theta_j)} \underset{\mathcal{H}_0}{\overset{\mathcal{H}_1}{\gtrless}} \eta, \quad (50)$$

where θ_j is the AOA of the jammer and $\mathbf{U}_j \in \mathbb{C}^{N \times (N-1)}$ is a slice of unitary matrix such that $\mathbf{P}_j^\perp = \mathbf{U}_j \mathbf{U}_j^\dagger$ with $\mathbf{P}_j^\perp = \mathbf{I}_N - \frac{\mathbf{v}(\theta_j) \mathbf{v}(\theta_j)^\dagger}{\mathbf{v}(\theta_j)^\dagger \mathbf{v}(\theta_j)}$. The curves for the likelihood ratio test with known parameters, referred to as clairvoyant detector (CD), are also included since they represent an upper bound to the detection performance.

In the next subsection, we focus on the stopping criterion and provide suitable numerical examples aimed at establishing a reasonable iteration number for both cyclic optimization procedures.

A. Selection of the Maximum Number of Iterations

The detection performance, assessed in Subsection IV-B, are obtained using a preassigned number of iterations. Now, in order to select this value, in Figs. 3 and 4, we show the average norm of the difference between the estimates at the n th iteration and their respective values at the $(n - 1)$ th iteration. The averages are evaluated over 1000 independent Monte Carlo trials assuming $N = 8$, $K = 12$, and $\text{SCNR} = 20$ dB. In both cases we model \mathbf{q} as a narrowband plane wave impinging onto the antenna array from a direction whose azimuth, generated at random at each Monte Carlo trial, is uniformly distributed outside the antenna mainlobe. Inspection of the figures highlights that 10 iterations for each procedure ensure a variation of the estimated quantities less than or equal to 10^{-5} and also represent a good compromise

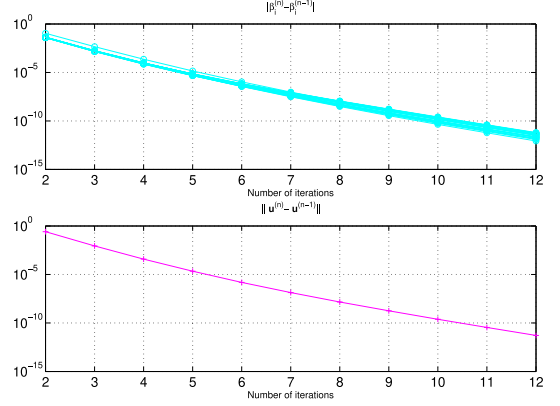


Fig. 4. Euclidean norm (or modulus) of the difference between the estimates at the n th iteration and those at the $(n - 1)$ th iteration versus the number of iterations for cyclic optimization of Subsection III-B.

TABLE II
CFAR ANALYSIS WITH RESPECT TO THE JAMMER POWER

JNR [dB]	25	30	35	40
R-NCP-D	0.001116	0.001158	0.001158	0.001167
D-NCP-D	0.001106	0.001142	0.001150	0.001145

TABLE III
CFAR ANALYSIS WITH RESPECT TO THE CLUTTER POWER

CNR [dB]	15	20	25	30
R-NCP-D	0.001158	0.001158	0.001126	0.001000
D-NCP-D	0.001146	0.001142	0.001122	0.001007

TABLE IV
CFAR ANALYSIS WITH RESPECT TO THE JAMMER AOA

AOA [deg]	25	45	55	65
R-NCP-D	0.001137	0.001124	0.001139	0.001205
D-NCP-D	0.001116	0.001107	0.001120	0.001197

from the computational point of view. For this reason, in what follows we adopt this number for the computation of the P_d curves.

B. Detection Performance

In this subsection, we investigate the behavior of the proposed architectures in terms of P_{fa} sensitivity to the interference parameters and P_d versus the SCNR for two different scenarios, which are complementary. Specifically, the former assumes a jammer illuminating the victim radar from its sidelobes, whereas the latter consider a surveillance area free of intentional interferers. It is important to underline that the second case does not correspond to the design assumptions.

The sensitivity analysis results for the P_{fa} with respect to jammer AOA, JNR, and CNR are summarized in Tables II–IV. Specifically, they are obtained by setting the threshold for a nominal scenario with $P_{fa} = 10^{-3}$ and estimating the actual P_{fa} under several instances of NCP power, NCP AOA, and clutter power. The values reported in the tables show that the actual P_{fa} of the proposed architectures does not experience a

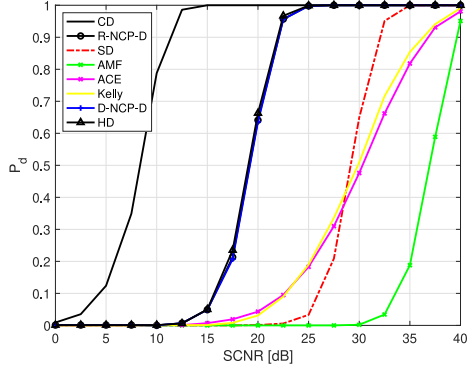


Fig. 5. P_d versus SCNR assuming $N = 8$, $K = 12$, and a jammer at 35° .

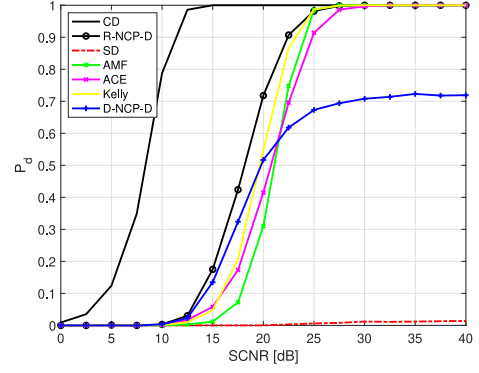


Fig. 8. P_d versus SCNR assuming $N = 8$, $K = 12$, and no jammers.

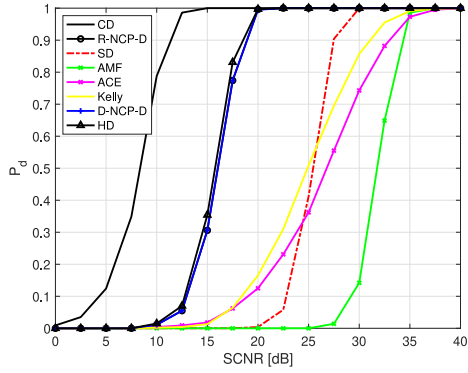


Fig. 6. P_d versus SCNR assuming $N = 8$, $K = 16$, and a jammer at 35° .

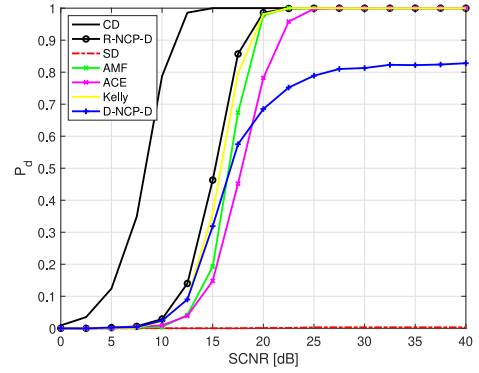


Fig. 9. P_d versus SCNR assuming $N = 8$, $K = 16$, and no jammers.

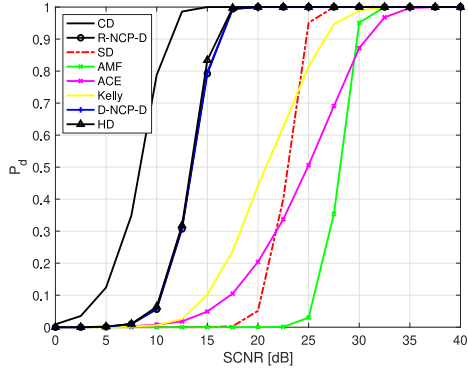


Fig. 7. P_d versus SCNR assuming $N = 8$, $K = 24$, and a jammer at 35° .

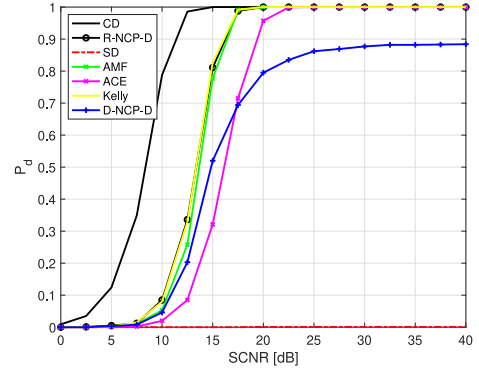


Fig. 10. P_d versus SCNR assuming $N = 8$, $K = 24$, and no jammers.

significant variation with respect to the nominal value, namely 10^{-3} , when the interference parameters take on value in the considered intervals. The observed trend suggests a method of practical appeal to set the detection thresholds. In fact, the latter can be computed resorting to a nominal scenario where the parameters are set using reference values.

Figs. 5–7 refer to the first scenario assuming $N = 8$ and different values for K . The common denominator of these figures is that R-NCP-D, D-NCP-D, and HD (which perfectly knows the jammer AOA) share the same performance, since the respective curves are overlapped, and outperform the remaining architectures except for the CD (as expected). The gain of the R-NCP-D and D-NCP-D over the SD is about 10 dB at $P_d = 0.9$. On the other hand, the AMF has the worst performance with a

loss at $P_d = 0.9$ ranging from about 7 dB for $K = 12$ to about 5 dB for $K = 24$ with respect to the SD. The curves of ACE and Kelly's GLRT are in between those of SD and AMF and intersect the latter. Comparison of the figures also points out that the P_d curves move towards left as K increases, which means that the P_d is an increasing function of K given the SCNR. Finally, the loss at $P_d = 0.9$ of the R-NCP-D/D-NCP-D with respect to the CD halves when K goes from $K = 12$, which corresponds to a loss of about 8 dB, to $K = 24$, which results in a loss of about 4 dB.

The second scenario is accounted for in Figs. 8–10, which assume the same parameter setting as previous figures except for the presence of the jammer. Note that the figures do not contain the P_d curve of HD since it cannot be used in this

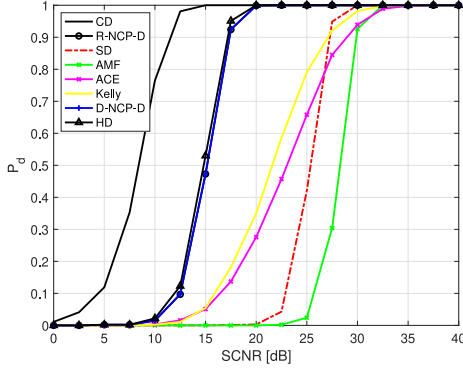


Fig. 11. P_d versus SCNR assuming $N = 16$, $K = 32$, and a jammer at 35° .

scenario because the information about the jammer AOA is not available. In this case, the curves of R-NCP-D and D-NCP-D are no longer overlapped and, more important, the latter does not achieve $P_d = 1$ at least for the considered parameter values. The R-NCP-D continues to provide satisfactory performance outperforming the other counterparts. In fact, the comparison with previous figures highlights that the performance of R-NCP-D keeps more or less unaltered. On the other hand, for the considered parameter values (and the considered scenario), the SD is completely useless since the resulting P_d values are close to zero, while the AMF and Kelly's GLRT significantly improve their performance as K increases ensuring about the same P_d values of the R-NCP-D for $K = 3N$.

Finally, the comparison between Fig. 11 and Fig. 6 allows to appreciate the performance variations due to both N and K when their ratio is constant. In fact, Fig. 11 assumes $N = 16$ and $K = 32$, namely twice the analogous values of Fig. 6. It can be noted that all the considered architectures except for the SD provide higher P_d values than those of Fig. 6; the performance of SD seems insensitive to the considered parameter change.

Summarizing, the above analysis singles out the R-NCP-D as an effective mean to face attacks of smart NLJs which transmit noise-like signals to cover the skin echoes from the platform under protection. As a matter of fact, the R-NCP-D outperforms all the other competitors either in the presence or absence of a noise cover pulse.

V. CONCLUSION

In this paper, two new detection architectures to account for possible NCP attacks have been proposed and assessed. Specifically, the first approach consists in modeling the NLJ contribution as a covariance component, while the second solution considers the realizations of the NLJ and handles them as deterministic signals. Ad hoc modifications of the GLRT have been devised for both scenarios where the unknown parameters are computed through alternating estimation procedures. The behavior of the two architectures has been first investigated resorting to simulated data adhering the design assumptions of the first approach and, then, they have been tested on data where the NCP is turned off. The analysis has singled out the R-NCP-D obtained with the first approach as the recommended solution

for adaptive detection in the presence of clutter and NCP, since it can guarantee satisfactory performance in both the considered situations at the price of an additional computational load with respect to its competitors due to the iterations necessary to reach a stationary point through the alternating maximization.

Finally, future research tracks might encompass the application of the herein presented approach to the case of range-spread targets possibly embedded in non-Gaussian clutter.

APPENDIX A

ALTERNATIVE DERIVATION OF THE AMF

In this Appendix, we modify the derivation contained in Subsection III-B by imposing the constraint $\mathbf{u}^\dagger \mathbf{v}_0 = 0$, namely the target steering vector and the NCP signature are orthogonal in the whitened space. For the reader convenience, let us recall that $\mathbf{u} = \mathbf{M}^{-1/2} \mathbf{q}$, $\mathbf{S}_1 = [\mathbf{x}_i \mathbf{x}_i^\dagger + \sum_{i \in \Omega \setminus \{\bar{i}\}} \mathbf{x}_i \mathbf{x}_i^\dagger]$, $\mathbf{v}_0 = \mathbf{M}^{-1/2} \mathbf{v}$, $\mathbf{x}_i = \mathbf{M}^{-1/2} \mathbf{z}_i$, $\mathbf{x}_{\bar{i}} = \mathbf{M}^{-1/2} \mathbf{z}_{\bar{i}}$.

Now, under \mathcal{H}_0 , the maximization with respect to β and β_i of w (given by (34)) leads to (35) and (36), respectively. Thus, assuming the orthogonality constraint, it is possible to reformulate the maximization of w with respect to \mathbf{u} as

$$\max_{\mathbf{u}: \mathbf{u}^\dagger \mathbf{v}_0 = 0} \exp \left\{ \frac{\mathbf{u}^\dagger \mathbf{S}_1 \mathbf{u}}{\mathbf{u}^\dagger \mathbf{u}} - \text{Tr} [\mathbf{S}_1] \right\}. \quad (51)$$

Let $\mathbf{U} \in \mathbb{C}^{N \times N-1}$ be a slice of unitary matrix, namely $\mathbf{U}^\dagger \mathbf{U} = \mathbf{I}_{N-1}$, with columns forming a basis for the orthogonal complement of the subspace spanned by \mathbf{v}_0 . Given the orthogonality constraint, it follows that \mathbf{u} can be expressed in terms of a linear combination of the columns of \mathbf{U} , i.e., $\mathbf{u} = \mathbf{U} \boldsymbol{\gamma}$ with $\boldsymbol{\gamma} \in \mathbb{C}^{(N-1) \times 1}$ the coordinate vector. Then, maximization (51) can be recast as

$$\begin{aligned} & \max_{\mathbf{u}: \mathbf{u}^\dagger \mathbf{v}_0 = 0} \exp \left\{ \frac{\mathbf{u}^\dagger \mathbf{S}_1 \mathbf{u}}{\mathbf{u}^\dagger \mathbf{u}} - \text{Tr} [\mathbf{S}_1] \right\} \\ &= \exp \left\{ \max_{\boldsymbol{\gamma}} \frac{\boldsymbol{\gamma}^\dagger \mathbf{U}^\dagger \mathbf{S}_1 \mathbf{U} \boldsymbol{\gamma}}{\boldsymbol{\gamma}^\dagger \boldsymbol{\gamma}} - \text{Tr} [\mathbf{S}_1] \right\} \\ &= \exp \left\{ \lambda_1 (\mathbf{U}^\dagger \mathbf{S}_1 \mathbf{U}) - \text{Tr} [\mathbf{S}_1] \right\}, \end{aligned} \quad (52)$$

where the last equality is due to the Rayleigh-Ritz theorem [31]. Thus, the solution to the constrained optimization problem, under \mathcal{H}_0 , is

$$\begin{aligned} & \max_{\beta, \beta_i, i \in \Omega \setminus \{\bar{i}\}, \mathbf{q}} \mathcal{L}_0(\beta, \beta_i, i \in \Omega \setminus \{\bar{i}\}, \mathbf{M}, \mathbf{q}) \\ &= \frac{1}{[\pi^N \det(\mathbf{M})]^H} \exp \left\{ \lambda_1 (\mathbf{U}^\dagger \mathbf{S}_1 \mathbf{U}) - \text{Tr} [\mathbf{S}_1] \right\}. \end{aligned} \quad (53)$$

On the other hand, under \mathcal{H}_1 , we can start from the partially-compressed likelihood with respect to α , given by (41). In fact, it is possible to show that, after optimization of the likelihood function with respect to α , β , and β_i , we obtain

$$\begin{aligned} & \max_{\alpha, \beta, \beta_i, i \in \Omega \setminus \{\bar{i}\}, \mathbf{q}} \mathcal{L}_1(\alpha, \beta, \beta_i, i \in \Omega \setminus \{\bar{i}\}, \mathbf{M}, \mathbf{q}) \\ &= \frac{1}{[\pi^N \det(\mathbf{M})]^H} \exp \left\{ \frac{\mathbf{u}^\dagger \mathbf{P}_{\mathbf{v}_0}^\perp \mathbf{x}_{\bar{i}} \mathbf{x}_{\bar{i}}^\dagger \mathbf{P}_{\mathbf{v}_0}^\perp \mathbf{u}}{\mathbf{u}^\dagger \mathbf{P}_{\mathbf{v}_0}^\perp \mathbf{u}} \right\} \end{aligned}$$

$$\begin{aligned}
& + \sum_{i \in \Omega \setminus \{\bar{i}\}} \frac{\mathbf{x}_i^\dagger \mathbf{u} \mathbf{u}^\dagger \mathbf{x}_i}{\mathbf{u}^\dagger \mathbf{u}} - \left(\mathbf{x}_i^\dagger \mathbf{P}_{v_0}^\perp \mathbf{x}_i + \sum_{i \in \Omega \setminus \{\bar{i}\}} \mathbf{x}_i^\dagger \mathbf{x}_i \right) \Bigg\} \\
& = \frac{1}{[\pi^N \det(\mathbf{M})]^H} \exp \left\{ \frac{\mathbf{u}^\dagger \mathbf{S}_1 \mathbf{u}}{\mathbf{u}^\dagger \mathbf{u}} - \left(\mathbf{x}_i^\dagger \mathbf{P}_{v_0}^\perp \mathbf{x}_i \right. \right. \\
& \quad \left. \left. + \sum_{i \in \Omega \setminus \{\bar{i}\}} \mathbf{x}_i^\dagger \mathbf{x}_i \right) \right\} \quad (54)
\end{aligned}$$

where the last equality comes from the orthogonality condition between \mathbf{u} and v_0 . Thus, it follows that

$$\begin{aligned}
& \max_{\mathbf{u}: \mathbf{u}^\dagger v_0 = 0} \max_{\alpha, \beta, \beta_i, i \in \Omega \setminus \{\bar{i}\}} \mathcal{L}_1(\alpha, \beta, \beta_i, i \in \Omega \setminus \{\bar{i}\}, \mathbf{M}, \mathbf{q}) \\
& = \frac{1}{[\pi^N \det(\mathbf{M})]^H} \\
& \quad \times \exp \left\{ \lambda_1(\mathbf{U}^\dagger \mathbf{S}_1 \mathbf{U}) - \left(\mathbf{x}_i^\dagger \mathbf{P}_{v_0}^\perp \mathbf{x}_i + \sum_{i \in \Omega \setminus \{\bar{i}\}} \mathbf{x}_i^\dagger \mathbf{x}_i \right) \right\} \quad (55)
\end{aligned}$$

where, again, the last equality comes from [31]. The final expression for the constrained GLRT-based architecture is obtained combining (53) and (55). Precisely, taking the log-likelihoods, the “constrained test (33)” is statistically equivalent to

$$\mathbf{x}_i^\dagger \mathbf{P}_{v_0}^\perp \mathbf{x}_i \underset{\mathcal{H}_0}{\overset{\mathcal{H}_1}{\geq}} \eta, \quad (56)$$

whose decision statistic, after replacing \mathbf{M} with the sample covariance matrix based on secondary data, coincides with that of the AMF.

REFERENCES

- [1] W. L. Melvin and J. A. Scheer, *Principles of Modern Radar: Advanced Techniques*. Edison, NJ, USA: Scitech Publishing, 2013.
- [2] A. Farina, *Antenna-Based Signal Processing Techniques for Radar Systems*. Boston, MA, USA: Artech House, 1992.
- [3] A. Farina, “Electronic counter-countermeasures,” in *Radar Handbook*, 3rd ed., M. Skolnik, Ed. McGraw-Hill, 2008, ch 24.
- [4] D. Adamy, *EW101: A First Course in Electronic Warfare*. Norwood, MA, USA: Artech House, 2001.
- [5] M. Greco, F. Gini, A. Farina, and V. Ravenni, “Effect of phase and range gate pull-off delay quantisation on jammer signal,” *IEE Proc.—Radar, Sonar Navigat.*, vol. 153, no. 5, pp. 454–459, Oct. 2006.
- [6] G. De Vito, A. Farina, R. Sanzullo, and L. Timmoneri, “Comparison between two adaptive algorithms for cancellation of noise like and coherent repeater interference,” in *Proc. Int. Symp. Radar*, Munich, Germany, Sep. 15–17, 1998, pp. 1385–1391.
- [7] A. Farina, L. Timmoneri, and R. Tosini, “Cascading SLB and SLC devices,” *Signal Process.*, vol. 45, no. 2, pp. 261–266, Aug. 1995.
- [8] S. Z. Kalson, “An adaptive array detector with mismatched signal rejection,” *IEEE Trans. Aerosp. Electron. Syst.*, vol. 28, no. 1, pp. 195–207, Jan. 1992.
- [9] C. D. Richmond, “The theoretical performance of a class of space-time adaptive detection and training strategies for airborne radar,” in *Proc. 32nd Annu. Asilomar Conf. Signals, Syst., Comput.*, Pacific Grove, CA, USA, Nov. 1–4, 1998, vol. 2, pp. 1327–1331.
- [10] N. B. Pulsone and M. A. Zatman, “A computationally-efficient two-step implementation of the GLRT,” *IEEE Trans. Signal Process.*, vol. 48, no. 3, pp. 609–616, Mar. 2000.
- [11] C. D. Richmond, “Performance of the adaptive sidelobe blanker detection algorithm in homogeneous clutter,” *IEEE Trans. Signal Process.*, vol. 48, no. 5, pp. 1235–1247, May 2000.
- [12] C. D. Richmond, “Performance of a class of adaptive detection algorithms in nonhomogeneous environments,” *IEEE Trans. Signal Process.*, vol. 48, no. 5, pp. 1248–1262, May 2000.
- [13] A. De Maio, “Robust adaptive radar detection in the presence of steering vector mismatches,” *IEEE Trans. Aerosp. Electron. Syst.*, vol. 41, no. 4, pp. 1322–1337, Oct. 2005.
- [14] F. Bandiera, A. De Maio, and G. Ricci, “Adaptive CFAR radar detection with conic rejection,” *IEEE Trans. Signal Process.*, vol. 55, no. 6, pp. 2533–2541, Jun. 2006.
- [15] O. Besson, “Detection of a signal in linear subspace with bounded mismatch,” *IEEE Trans. Aerosp. Electron. Syst.*, vol. 42, no. 3, pp. 1131–1139, Jul. 2006.
- [16] A. De Maio, “Rao test for adaptive detection in Gaussian interference with unknown covariance matrix,” *IEEE Trans. Signal Process.*, vol. 55, no. 7, pp. 3577–3584, Jul. 2007.
- [17] M. Greco, F. Gini, and A. Farina, “Radar detection and classification of jamming signals belonging to a cone class,” *IEEE Trans. Signal Process.*, vol. 56, no. 5, pp. 1984–1993, May 2008.
- [18] F. Bandiera, D. Orlando, and G. Ricci, “A subspace-based adaptive sidelobe blanker,” *IEEE Trans. Signal Process.*, vol. 56, no. 9, pp. 4141–4151, Sep. 2008.
- [19] F. Bandiera, O. Besson, D. Orlando, and G. Ricci, “An improved adaptive sidelobe blanker,” *IEEE Trans. Signal Process.*, vol. 56, no. 9, pp. 4152–4161, Sep. 2008.
- [20] F. Bandiera, D. Orlando, and G. Ricci, “Advanced radar detection schemes under mismatched signal models,” *Synthesis Lectures on Signal Processing*. San Rafael, CA, USA: Morgan & Claypool, Mar. 2009.
- [21] F. Bandiera, A. Farina, D. Orlando, and G. Ricci, “Detection algorithms to discriminate between radar targets and ECM signals,” *IEEE Trans. Signal Process.*, vol. 58, no. 12, pp. 5984–5993, Dec. 2010.
- [22] F. Bandiera, O. Besson, and G. Ricci, “An ABORT-like detector with improved mismatched signals rejection capabilities,” *IEEE Trans. Signal Process.*, vol. 56, no. 1, pp. 14–25, Jan. 2008.
- [23] F. Bandiera, A. De Maio, A. S. Greco, and G. Ricci, “Adaptive radar detection of distributed targets in homogeneous and partially homogeneous noise plus subspace interference,” *IEEE Trans. Signal Process.*, vol. 55, no. 4, pp. 1223–1237, Apr. 2007.
- [24] W. Liu, J. Liu, H. Li, Q. Du, and Y. Wang, “Multichannel signal detection based on wald test in subspace interference and Gaussian noise,” *IEEE Trans. Aerosp. Electron. Syst.*, vol. 55, no. 3, pp. 1370–1381, Jun. 2019.
- [25] A. Coluccia and G. Ricci, “ABORT-like detection strategies to combat possible deceptive ECM signals in a network of radars,” *IEEE Trans. Signal Process.*, vol. 63, no. 11, pp. 2904–2914, Jun. 2015.
- [26] L. B. Van Brunt, *Applied ECM*, vol. 2. Riverside, CA, USA: EW Engineering, 1982.
- [27] E. Conte, A. De Maio, and G. Ricci, “Recursive estimation of the covariance matrix of a compound-Gaussian process and its application to adaptive CFAR detection,” *IEEE Trans. Signal Process.*, vol. 50, no. 8, pp. 1908–1915, Aug. 2002.
- [28] P. Stoica and Y. Selen, “Cyclic minimizers, majorization techniques, and the expectation-maximization algorithm: A refresher,” *IEEE Signal Process. Mag.*, vol. 21, no. 1, pp. 112–114, Jan. 2004.
- [29] A. De Maio, D. Orlando, C. Hao, and G. Foglia, “Adaptive detection of point-like targets in spectrally symmetric interference,” *IEEE Trans. Signal Process.*, vol. 64, no. 12, pp. 3207–3220, Jun. 15, 2016.
- [30] A. Coluccia and G. Ricci, “Adaptive radar detectors for point-like Gaussian targets in Gaussian noise,” *IEEE Trans. Aerosp. Electron. Syst.*, vol. 53, no. 3, pp. 1284–1294, Jun. 2017.
- [31] R. A. Horn and C. R. Johnson, *Matrix Analysis*. Cambridge, U.K.: Cambridge Univ. Press, 1985.
- [32] H. L. Van Trees, *Optimum Array Processing (Detection, Estimation, and Modulation Theory, Part IV)*. Hoboken, NJ, USA: Wiley, 2002.
- [33] F. C. Robey, D. L. Fuhrman, E. J. Kelly, and R. Nitzberg, “A CFAR adaptive matched filter detector,” *IEEE Trans. Aerosp. Electron. Syst.*, vol. 29, no. 1, pp. 208–216, Jan. 1992.
- [34] E. Conte, M. Lops, and G. Ricci, “Asymptotically optimum radar detection in compound Gaussian noise,” *IEEE Trans. Aerosp. Electronic Syst.*, vol. 31, no. 2, pp. 617–625, Apr. 1995.
- [35] S. Kraut and L. L. Scharf, “The CFAR adaptive subspace detector is a scale-invariant GLRT,” *IEEE Trans. Signal Process.*, vol. 47, no. 9, pp. 2538–2541, Sep. 1999.
- [36] E. J. Kelly, “An adaptive detection algorithm,” *IEEE Trans. Aerosp. Electron. Syst.*, vol. AES-22, no. 2, pp. 115–127, Mar. 1986.



Pia Addabbo (M'09) received the B.Sc. and M.Sc. degrees in telecommunication engineering, and the Ph.D. degree in information engineering from the University of Sannio, Benevento, Italy, in 2005, 2008, and 2012, respectively. She is currently a Researcher with the "Giustino Fortunato" University, Benevento, Italy. Her research interests include statistical signal processing applied to radar target recognition, global navigation satellite system reflectometry, and hyperspectral unmixing. She is a coauthor of scientific publications in international journals and conferences.



Olivier Besson received the Ph.D. degree in signal processing from Institut National Polytechnique Toulouse, Toulouse, France, in 1992. He is currently a Professor with Institut Supérieur de l'Aéronautique et de l'Espace (ISAE-SUPAERO), Toulouse, France. His research interests include statistical array processing, multivariate analysis, adaptive detection, and estimation.



Danilo Orlando (SM'13) was born in Gagliano del Capo, Italy, on August 9, 1978. He received the Dr. Eng.(Hons.) degree in computer engineering and the Ph.D. degree (with maximum score) in information engineering, both from the University of Salento (formerly University of Lecce), Lecce, Italy, in 2004 and 2008, respectively. From July 2007 to July 2010, he has worked with the University of Cassino, Cassino, Italy, engaged in a research project on algorithms for track-before-detect of multiple targets in uncertain scenarios. From September to November 2009, he has

been a Visiting Scientist with the NATO Undersea Research Centre (NURC), La Spezia, Italy. From September 2011 to April 2015, he has worked with the Elettronica SpA engaged as system analyst in the field of Electronic Warfare. In May 2015, he joined Università degli Studi "Niccolò Cusano," where he is currently working as an Associate Professor. His main research interests are in the field of statistical signal processing with more emphasis on adaptive detection and tracking of multiple targets in multisensor scenarios. He has held visiting positions with the Department of Avionics and Systems, ENSICA (now Institut Supérieur de l'Aéronautique et de l'Espace, ISAE), Toulouse, France, in 2007 and with the Chinese Academy of Science, Beijing, China, in 2017–2019. He is also an author or coauthor of more than 100 scientific publications in international journals, conferences, and books. He is a Senior Area Editor for the IEEE TRANSACTIONS ON SIGNAL PROCESSING, and an Associate Editor for the IEEE OPEN JOURNAL ON SIGNAL PROCESSING, *EURASIP Journal on Advances in Signal Processing*, and *MDPI Remote Sensing*.



Giuseppe Ricci (M'01–SM'10) was born in Naples, Italy, on February 15, 1964. He received the Dr. Eng. and Ph.D. degrees in electronic engineering from the University of Naples "Federico II," Naples, Italy, in 1990 and 1994, respectively. Since 1995, he has been with the University of Salento (formerly University of Lecce), Lecce, Italy, first as an Assistant Professor of Telecommunications and, since 2002, as a Professor. He has held visiting positions with the University of Colorado, Boulder, CO, USA, from 1997 to 1998 and in April/May 2001, with the Colorado State University, Fort Collins, CO, USA, in July/September 2003, March 2005, September 2009, and March 2011, with Ensica, Toulouse, France, in March 2006, and with the University of Connecticut, Storrs, CT, USA, in September 2008. His research interests are in the field of statistical signal processing with emphasis on radar processing, localization algorithms, and CDMA systems. More precisely, he has focused on high-resolution radar clutter modeling, detection of radar signals in Gaussian and non-Gaussian disturbance, oil spill detection from SAR data, track-before-detect algorithms fed by space-time radar data, localization in wireless sensor networks, multiuser detection in overlay CDMA systems, and blind multiuser detection.